Calhoun: The NPS Institutional Archive

DSpace Repository

Theses and Dissertations | 1. Thesis and Dissertation Collection, all items

1962

Theoretical investigation of slamming loads on a three dimensional shape

Swanson, Harlan D.

Massachusetts Institute of Technology

http://hdl.handle.net/10945/13268

This publication is a work of the U.S. Government as defined in Title 17, United States Code, Section 101. Copyright protection is not available for this work in the United States.

Downloaded from NPS Archive: Calhoun

http://www.nps.edu/library

Calhoun is the Naval Postgraduate School's public access digital repository for research materials and institutional publications created by the NPS community. Calhoun is named for Professor of Mathematics Guy K. Calhoun, NPS's first appointed -- and published -- scholarly author.

Dudley Knox Library / Naval Postgraduate School
411 Dyer Road / 1 University Circle
Monterey, California USA 93943

NPS ARCHIVE
1962
SWANSON, H.

THEORETICAL INVESTIGATION OF SLAMMING LOADS ON A THREE DIMENSIONAL SHAPE

by Lt. Harlan D. Swanson, USN

Supervisor: Prof. M. A. Abkowitz

May 19, 1962

Thesis
S924

THEORETICAL INVESTIGATION OF SLAMMING LOADS ON A THREE DIMENSIONAL SHAPE

by

HARLAN D. SWANSON, LIEUTENANT, UNITED STATES NAVY
B. S., U. S. Naval Academy
(1956)

SUBMITTED IN PARTIAL FULFILLMENT OF THE REQUIREMENTS
FOR THE DEGREE OF NAVAL ENGINEER
AND THE DEGREE OF
MASTER OF SCIENCE IN NAVAL ARCHITECTURE AND
MARINE ENGINEERING at the
MASSACHUSETTS INSTITUTE OF TECHNOLOGY
May 1962

Signature of Author: .....
Department of Naval Architecture and
Marine Engineering, May 10, 1962

Certified by: .....
Thesis Supervisor

Accepted by: .....
Chairman, Departmental Committee
on Graduate Students

MIT ARCHIVE
2.62
SWANSON, H

Library
U.S. Naval Postgraduate School
Monterey, California

THEORETICAL INVESTIGATION OF SLAMMING LOADS ON A THREE DIMENSIONAL SHAPE

by

Harlan D. Swanson, U.S.N.

Submitted to the Department of Naval Architecture and Marine Engineering on May 19, 1962 in partial fulfillment of the requirements for the Master of Science degree in Naval Architecture and Marine Engineering and the professional degree, Naval Engineer.

ABSTRACT

This paper is an attempt to develop a method for determining the slamming pressures and loads on ship hulls, when the relative vertical velocity relationship between the wave slope and keel is specified. A basic two-dimensional theory for hydrodynamic impact is utilized which avoids linearization of the free surface. The mathematical model for the theoretical developement is a wedge. A method of analysis is presented which yields the free surface shape and pressures associated with symmetrical penetration of a fluid surface by wedges of varying deadrise angle. The anaylsis is based on the principles of continuity of fluid flow and similarity. The principle of continuity makes use of the fact that the volume of displaced water above the original water line. The principle of similarity accounts for the proportional expansion of the free surface with continued penetration of the body. The free surface (consisting of both wave and spray) is considered to be increasing in such a manner that the slope and velocity of the surface is determined by the position and penetration velocity of the impacting body. Once the correct free surface shape has been determined by a graphical iterative method, for any instant of time, the associated velocity potential and pressure can be determined numerically for various points on the body.

Since only V-shaped ship sections can be approximated by wedges, a method is developed by which the pressures on a U-shaped ship section of a low deadrise angle can be calculated. Results are presented which resulted from calculations carried out on a ship with low deadrise angles in the foward

sections. For comparison, a calculation was performed for a Liberty ship section which could be satisfactorily approximated by a straight wedge shape. Also, the integrated pressure load was determined for several instants of time for the ship being considered.

The results of the calculations seemed to give realistic values for the pressure distribution. However, the numerical calculations, as developed in this paper, are quite tedious. Computer solutions need to be developed. Also, the approximation of ship sections of low deadrise angles by blunt nose wedges is questionable, since the spray root thickness has to be approximated. Therefore, the free surface shape in the spray root area is an approximation. The theoretical results should be closely checked by experiments.

ACKNOWLEDGEMENTS

The author wishes to express his appreciation to Professor M. A. Abkowitz, Department of Naval Architecture and Marine Engineering, M.I.T., for his guidance in this work.

ACKNOWLEDGMENTS

The author wishes to express his appreciation to Professor M. A. Abkowitz, Department of Naval Architecture and Marine Engineering, M.I.T., for his guidance in this work.

TABLE OF CONTENTS

TABLE OF CONTENTS

LIST OF FIGURES

LIST OF FIGURES

NOTATION

Symbol	
a, b	Points on the free surface
c	Nominal wetted half width of the impacting body (ft.)
g	Acceleration due to gravity (ft/sec.^{2})
h	Wave height (double amplitude) (ft.)
H	Normal draft (ft.)
L	Ship length (ft.)
O	Origin of coordinate systems
O'	Edge of spray; origin for s
P	Pressure at any point in flow field (lb/in^2)
r	Distance from origin to point in fluid (ft.)
r_m	Wave amplitude (ft.)
R	Amplitude of complex number
s, S	Distance along free surface curve from its origin at the solid boundary (ft.)
t	Time (sec.)
Te	Period of encounter between waves and ship
u	Velocity component in x-direction (ft/sec)
U	Resultant velocity at any point in fluid $=\sqrt{v^2 + w^2}$ (ft/sec)
v	Velocity component in y-direction (ft/sec)
V	Ship speed (ft/sec)
V_n	Water surface velocity relative to model bottom (or flat plate); a function of $y > c$ (ft/sec)
w	Velocity component in z-direction (ft/sec)
x, y, z	Linear displacements of center of gravity of ship along fixed axes
X, Y, Z	Coordinate system fixed in ship
z_m	Heave amplitude

NOTATION

Symbol	
a, b	Points on the free surface
c	Maximum vertical half width of the impacting body (ft.)
g	Acceleration due to gravity (ft/sec.^{2})
h	Wave height (double amplitude) (ft.)
H	Normal head (ft.)
L	Half length (ft.)
O	Origin of coordinate system
p_s	Shape of spray; origin for s
p	Pressure at any point in flow field (lb/in^2)
r	Distance from origin to point in fluid (ft.)
r_m	Wave amplitude (ft.)
R	Amplitude of complex number
s, s_1	Distance along free surface curve from its origin at the solid boundary (ft.)
t	Time (sec.)
Te	Period of interval between wave and slip
u	Velocity component in x-direction (ft/sec)
U	Resultant velocity at any point in fluid $\sqrt{u^2 + w^2}$ (ft/sec)
v	Velocity component in y-direction (ft/sec)
V	Slip speed (ft/sec)
V_n	Water surface velocity relative to moving bottom (at flat plate); a function of $y > c$ (ft/sec)
w	Velocity component in z-direction (ft/sec)
x, y, z	Linear displacements of center of gravity of slip along fixed axes
X, Y, Z	Coordinate system fixed in slip
z_m	Wave amplitude

z_x	Relative position of ship keel with respect to water surface (ft)
$\dot{z}_x$	Relative velocity of keel with respect to water surface; penetration velocity (ft/sec)
α	Angle between velocity vector, U, and radius r
β	Deadrise angle
γ	Angle between radial velocity and the surface velocity past the radius
δ	Spray root thickness; phase angle for heave
ϵ	Phase angle for pitch
η	z-coordinate of particular fluid particle
λ	Wave length (ft)
ξ	y-coordinate of a particular fluid particle
ρ	Mass density of fluid $(\frac{lb\ sec^2}{ft^4})$
ψ	Pitch angle
ψ_m	Pitch amplitude
ω_e	Frequency of encounter between the ship and waves (rad/sec)

I. INTRODUCTION

In recent years there has been a distinct trend toward increasing the speed and displacement of ships. Quite often a ship's speed is not governed by its installed horsepower, but by its response to the seaway. The term "response" includes not only the ship's motion, but also the effect on the ship's structure caused by the motion. One possible result of a ship's motion in a seaway is the slamming force exerted on the forward portion of the hull structure. The force is usually caused by the emergence of the bow and subsequent impact with the water on reentry. The ship may vibrate for some time after such an impact, and plates on the bottom shell may be damaged. If the impacts are severe enough, serious structural damage may occur, and even if the blows are of small magnitude, but frequent, the hull will possibly be weakened by fatigue.

The earliest theoretical work on slamming loads resulted from studies on the impacts sustained by seaplanes when they landed. The quantitative evaluation of the impact forces was based on the "expanding plate" and "spray root" theories. The expanding plate theory originated with Von Karman in 1929 (1) *. By this theory, the water flow pattern around a wedge penetrating the water surface is taken to be equivalent at each instant to the flow about a flat plate of the same width as the wetted width of the wedge. From this analysis, the velocities, accelerations, and resultant pressures and hydrodynamic reactions are obtained. Apparently Von Karman's theory is good for low deadrise angles, but is only a crude approximation at higher angles (2). By the spray root theory, developed by Wagner in 1932, the local flow phenomena occuring

*) Numbers in brackets refer to bibliography.

1. INTRODUCTION

In recent years there has been a distinct trend toward increasing the speed and displacement of ships. Quite often a ship's speed is but governed by its installed horsepower, but by its response to the seaway. The term "response" includes not only the ship's motions, but also the effect on the ship's structures caused by the motion. One possible result of a ship's motion, in a seaway is the slamming force exerted on the forward portion of the hull structure. The force is usually caused by the emergence of the bow and subsequent impact with the water on reentry. The ship may vibrate for some time after such an impact, and plates on the bottom shell may be damaged. If the impacts are severe enough, serious structural damage may occur, and even if the blows are of small magnitude, but frequent, the hull will possibly be weakened by fatigue.

The earlier theoretical work on slamming loads resulted from studies on the impacts experienced by seaplanes when they landed. The quantitative evaluation of the impact forces was based on the "expanding plate" and "spray root" theories. The expanding plate theory originated with Von Karman in 1929 (1) *. By this theory, the water flow pattern around a wedge penetrating the water surface is taken to be equivalent at each instant to the flow about a flat plate of the same width as the vertical width of the wedge. From this analysis, the velocities, accelerations, and resultant pressures and hydrodynamic reactions are obtained. Apparently Von Karman's theory is good for low deadrise angles, but is only a crude approximation at higher angles (2). By the spray root theory, developed by Pierson in 1948, the local flow phenomena occurring

---

*) Numbers in brackets refer to bibliography.

at the edge of the wetted area is described. The high pressures that exist near the edge of the wetted area during impact are connected with the formation of a spray jet in which the water is quickly accelerated to a high velocity.

Seaplane impact theories have been adapted to the problems of ship slamming (3, 4) in an attempt to predict the pressure response of a given hull form. Experiments have been devised and carried out (4, 5, 6) utilizing ship models. The experimentations have been carried out under conditions allowing three dimensional flow about the ship hull, which are obviously the conditions met by ships at sea. However, three dimensional flow analysis for a general curved body is much more complex than that of two dimensional flow. Therefore, theoretical work has been primarily concerned with the flow about two dimensional ship sections of finite length. The slamming loads for the individual sections have been combined by strip theory to obtain the pressure distribution on the total area of the ship bottom affected by the slam.

There is a pressing need for the extension of the available two-dimensional water entry theories. In the expanding plate theory, the free surface is represented by a zero potential line. The impact of ship hull shape bodies on a water surface will usually result in the formation of a curved free surface, and a spray root. Theoretically the presence of a highly curved free surface may not be represented by a straight zero potential line. It seems likely that the free surface is nearly a horizontal line only for bodies of high deadrise angles, and that the spray root generated at low deadrise angles disputes the assumption of a horizontal zero potential line. In general, for any of the "fitting" techniques (ellipse and circle fitting as well as the expanding plate), the agreement between theory and experiment has been rather poor (2), even for simple wedge shaped bodies. Therefore, a more exact solution of the hydrodynamic impact problem would be desirable.

The object of this work is to formulate a basic two-dimensional theory for hydrodynamic impact which avoids linearization of the free-surface boundary condition, and which can be adapted to the ship impact problem. The theory is based largely on the work of Pierson (7) who developed an iterative numerical solution for a wedge entering the water at constant velocity. While a wedge is used as the mathematical model in this paper, the velocity is not considered to be constant.

The problem of determing slamming pressures actually consists of two parts; first, the description of the ship motion in a seaway which leads to slamming, and second, the description of the pressures and forces on the hull caused by slamming. Ship motions are not treated here, but an expression for ship motion is needed to determine, at any instant, the relative vertical velocity of the ship with respect to the water surface. Such an expression was obtained from experimental work for a Liberty type ship, discussed in reference (3).

Because of the difficulty of analytically describing the flow about an arbitrary convex body, the expressions for the velocity potential derived in the paper are based on the water entry of a wedge. The deadrise angle of the wedge is taken to be approximately the same as the deadrise angle of the ship section under consideration. While the above assumption appears to be somewhat gross, in the light of past experimental and theoretical work it does not seem to be bad. Both experimental and theoretical calculations have shown that the highest transverse pressure distributions occur on a given ship section shortly after it hits the water (3, 6, 8). The theoretical calculations were based on the expanding plate theory, with a modification for the hull section curvature and added mass of water. However, the portion of the hull that experiences the largest pressure loading is the bottom portion which,

for most ships, is roughly equivalent to a wedge of low deadrise angle, or can at least be approximated (at least for the period just before and after slamming) by a wedge of a specified angle. It is not sufficient just to compute the pressure distribution at the instant of slamming, but pressure distributions for several instants before and after slamming are also required for a complete picture of the pressure loading. From a structural viewpoint, it is the pressure loading and its time variation which are important, and not peak pressures which last only for a few micro-seconds.

The development of the theory is presented in Chapter II. The results of the theory, as applied to a given ship for which other theoretical and experimental data are available, are presented and discussed in Chapters III and IV.

II. PROCEDURE

A. General The theoretical calculations are carried out for a ship approximately the size of a Liberty ship. The actual ship lines were calculated from the series of sections for which Professor F. M. Lewis obtained his values of inertia coefficients (9). Professor J. E. Kerwin obtained the offsets and polynomial expressions for the ship lines by the use of the 7090 IBM computer. Also, a calculation is performed for comparison for a section of the Liberty ship used in references (3, 4).

B. Determination of Ship Motion The coordinate system used for the determination of ship motion is the same one used in reference (10). The coordinate origin is taken to be at midships. The (x, y, z) coordinates represent linear displacements of the center of gravity along fixed axes. In this paper, only heaving and pitching motions are considered, therefore only the z coordinate is of interest. The z axis is vertical and z is positive upward. Of the three angular displacements (roll, pitch, and yaw), only the pitch angle is of interest. Positive indicates bow up. Also, the (X, Y, Z) coordinate system, which is related to the ship's principal axes, is introduced. The Z-coordinate is positive up, the X-coordinate positive forward, and the Y-coordinate positive to port. The pertinent coordinates and their positive directions are shown in Fig. 1.

In order to obtain a complete picture of the ship motion at any instant of time, it is necessary to know the instantaneous draft and relative velocity between the keel and water surface for any station.

The pitching motion is assumed to be

$$\psi = \psi_m \cos(\omega_e t + \epsilon)$$

II. DISCUSSION

A. General The theoretical calculations are carried out for a ship approximately the size of a Liberty ship. The natural ship lines were calculated from the basins of sections for which Prohaska [7, 8] Lewis obtained his values of inertia coefficients [9]. Prohaska [7, 8] Lewis obtained the offsets and polynomial approximations for the ship lines by the use of the 7090 IBM computer; also, a calculation is performed for comparison for a section of the Liberty ship used in reference [3, 4].

B. Determination of Ship Motion The coordinate system used for the determination of ship motion in the zoz x one used in reference [10]. The coordinate origin is taken to be at midships. The (X, Y, Z) coordinates represent linear displacements of the center of gravity along fixed axes. In this paper, only heaving and pitching motions are considered. Therefore only the z coordinate is of interest. The z axis is vertical and z is positive upward. Of the three angular displacements (roll, pitch, and yaw), only the pitch angle is of interest. Positive indicates bow up. Also, the (X, Y, Z) coordinate system, which is related to the ship's principal axes, is introduced. The Z-coordinate is positive up, the X-coordinate positive forward, and the Y-coordinate positive to port. The pertinent coordinates and their positive directions are shown in Fig. 1.

In order to obtain a complete picture of the ship motion at any instant of time, it is necessary to know the instantaneous displacement and relative velocity between the keel and water surface for any station.

The pitching motion is assumed to be

$$\psi = \psi_m \cos(\omega t + \varepsilon)$$

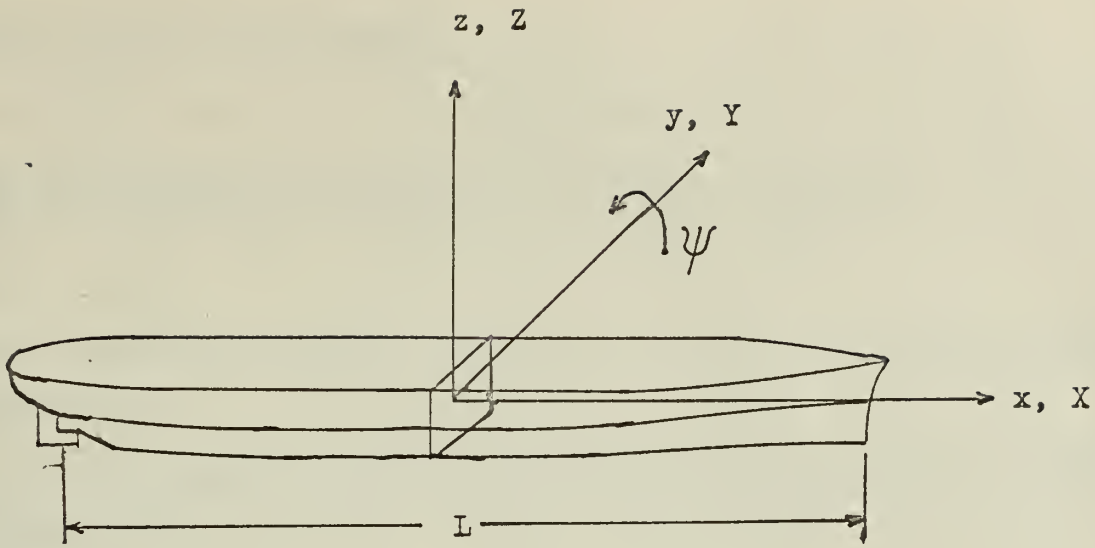

FIGURE I PRINCIPAL COORDINATES AND AXES OF REFERENCE

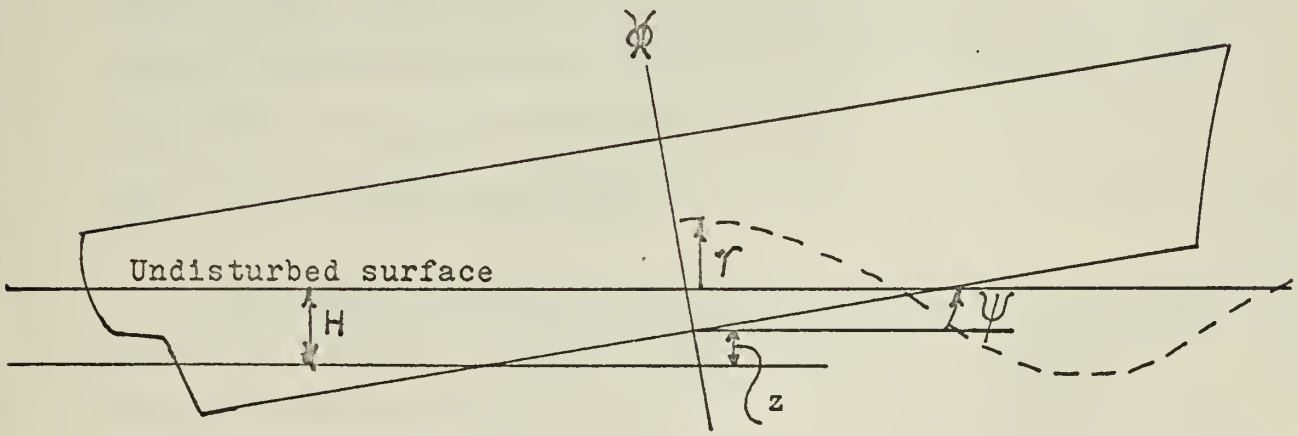

FIGURE II RELATIVE ELEVATION OF KEEL ABOVE DISTURBED WATER SURFACE

and the heave is assumed to be

$$z = z_m \cos(\omega_e t + \delta).$$

The wave elevation at any station along the ship is given by

$$\gamma = \gamma_m \cos\left(\frac{2\pi X}{\lambda} + \omega_e t\right)$$

where $\omega_e = \frac{2\pi}{\lambda}\left(V + \frac{\lambda g}{2\pi}\right)$ = period of encounter between ship and waves in head seas.

The relative position of the keel above the disturbed water surface is given by:

$$z_x = \gamma - z - X\psi + H \qquad (1)$$

for any station (see Figure II). Emergence is associated with $z_x < 0$.

The relative velocity between the ship and wave at a distance X from amidships is given by

$$\dot{z}_x = \dot{\gamma} - \dot{z} - X\dot{\psi} \qquad (2)$$

where $\dot{\gamma} = \frac{\partial \gamma}{\partial t} = -\omega_o \gamma_m \sin\left(\omega_e t + \frac{2\pi X}{\lambda}\right)$,

and ω_o is the absolute angular frequency of the wave and equals $\frac{2\pi g}{\lambda}$,

and $\dot{z} = \frac{\partial Z}{\partial t} = -z_m \omega_e \sin(\omega_e t + \ )$,

and $\dot{\psi} = \frac{\partial}{\partial t} = -\psi_m \omega_e \sin(\omega_e t + \epsilon)$.

From reference (11), experimental values of ∂ and were obtained for a 5.5 ft. model of a Liberty ship in regular waves of a specified height. The values given for the model are the same for the full scale ship, with the exception of the heave amplitude, which is scaled up for the ship by a ratio of the lengths. The pertinent variables for the model, full scale ship, and equivalent Lewis ship are tabulated in Table I.

The calculations of the relative velocity between the keel and the

and the heave is assumed to be

$$z = z_m \cos(\omega_e t + \delta).$$

The wave elevation at any station along the ship is given by

$$\zeta = \zeta_m \cos\left(\frac{2\pi X}{\lambda} + \omega_e t\right)$$

where $\omega_e = \frac{2\pi}{\lambda}\left(V + \sqrt{\frac{g\lambda}{2\pi}}\right)$ = period of encounter between ship and waves in head seas.

The relative position of the keel above the disturbed water surface is given by:

$$z_x = \zeta - z - X\psi + H \qquad (1)$$

for any station (see Figure II). Emergence is associated with $z_x > 0$.

The relative velocity between the ship and wave at a distance X from amidships is given by

$$\dot{z}_x = \dot{\zeta} - \dot{z} - X\dot{\psi} \qquad (2)$$

where $\dot{\zeta} = \frac{\partial \zeta}{\partial t} = -\omega_o \zeta_m \sin\left(\omega_e t + \frac{2\pi X}{\lambda}\right)$.

and ω_o is the absolute angular frequency of the wave and equals $\frac{2\pi g}{\lambda}$,

and $\dot{z} = \frac{\partial z}{\partial t} = -z_m \omega_e \sin(\omega_e t + \delta)$.

and $\dot{\psi} = \frac{\partial \psi}{\partial t} = -\psi_m \omega_e \sin(\omega_e t + \epsilon)$.

From reference (11), experimental values of δ and ϵ were obtained for a 5.5 ft. model of a Liberty ship in regular waves of a specified height. The values given for the model are the same for the full scale ship, with the exception of the heave amplitude, which is scaled up for the ship by a ratio of the lengths. The pertinent variables for the model, full scale ship, and equivalent Lewis ship are tabulated in Table I.

The calculations of the relative velocity between the keel and the

water by Eq. (2) will result in a sinusoidal variation of velocity for any station. While this is not correct, it is shown in reference (3) that this is a good approximation for the relative velocity of a ship subject to slamming motion in regular waves. In other words, the change in relative velocity due to slamming loads is very small.

Slamming, as generally defined, is the sudden change of the acceleration of the ship. While the relative velocity does not deviate much from that predicted by (2), the influence of slamming on the acceleration is quite marked (3). However, in this study of slamming, the pressures are governed by the velocity and penetration of the keel instead of the acceleration. For the ship hulls under consideration, the portions of the ship between stations 0 and 5 is subject to slamming. From reference (3) the instant of slamming is determined to be in the vicinity of t = 1.29 sec. The penetration, and relative velocities of stations 0 through 5 are graphed for the interval from t = 1.20 sec. to t = 1.44 sec. in Figs. III and IV. These values will be used to determine the slamming pressures on the forward portions of the ship. The values used to plot the curves in Figures III and IV were computed from equations (1a) and (1b) which resulted when the amplitudes and phase angles from Table I were substituted into equations (1) and (2).

$$z_x = -12.8 \cos\left(\omega_e t + \frac{2\pi X}{382}\right) - 5.35 \cos(\omega_e t - 0.623) - 0.122 X \cos(\omega_e t + 0.25 \quad (1a)$$

$$z_x = -9.3 \sin\left(\omega_e t + \frac{2\pi X}{382}\right) - 5.35 \sin(\omega_e t - .623) - .122 X \sin(\omega_e t + .252) \quad (1b)$$

C. Theoretical Analysis

Conditions of the Problem

1. The problem is treated as a two-dimensional one. The velocity potential and pressure distribution will be calculated for two-dimensional

water by Eq. (2) will result in a sinusoidal variation of velocity for any station. While this is not correct, it is shown in reference (3) that this is a good approximation for the relative velocity of a ship subject to slamming motion in regular waves. In other words, the change in relative velocity due to slamming loads is very small.

Slamming, as generally defined, is the sudden change of the acceleration of the ship. While the relative velocity does not deviate much from that predicted by (2), the influence of slamming on the acceleration is quite marked (3). However, in this study of slamming, the pressures are governed by the velocity and penetration of the keel instead of the acceleration. For the ship hulls under consideration, the portions of the ship between stations 0 and 5 is subject to slamming. From reference (3) the instant of slamming is determined to be in the vicinity of $t = 1.32$ sec. The penetration, and relative velocities of stations 0 through 5 are graphed for the interval from $t = 1.20$ sec. to $t = 1.44$ sec. in Figs. III and IV. These values will be used to determine the slamming pressures on the forward portions of the ship. The values used to plot the curves in Figures III and IV were computed from equations (10) and (11) which resulted when the amplitudes and phase angles from Table I were substituted into equations (1) and (2).

$$\dot{s}_x = -12.8\cos\left(\omega_e t + \frac{2\pi X}{510}\right) - 3.35\cos(\omega_e t - 0.825) + 0.1825X\cos(\omega_e t + 0.50 \quad (10)$$

$$s_x = -4.3\sin\left(\omega_e t + \frac{2\pi X}{365}\right) - 5.25\sin(\omega_e t - .652) - .122X\sin(\omega_e t + .5463) \quad (11)$$

C. Theoretical Analysis

Conditions of the Problem

1. The problem is treated as a two-dimensional one. The velocity potential and pressure distribution will be calculated for two-dimensional

TABLE I

	Model	Liberty ship	Lewis type ship
Length (BP) L, ft.	5.5	416.0	420.0
Beam, B, ft.	0.732	56.9	57.5
Draft, H, ft.	0.21	15.9	16.0
Scale factor	1.0	75.7	76.5
Speed V, knots	1.1	9.6	9.7
Wave length λ, ft.	5.0	379.0	382.0
Wave height h, ft.	0.334	25.3	25.5
Pitch amplitude ψ_m, degrees	7	7	7
Heave amplitude Z_m, ft.	0.007	5.30	5.35
Pitch phase ϵ, degrees	14.44	14.44	14.44
Heave phase δ, degrees	-35.7	-35.7	-35.7
Frequency of encounter ω_e, $\frac{\text{rad.}}{\text{sec.}}$	8.74	1.01	1.00
Period of encounter T_e, sec.	0.72	6.28	6.28
Wave frequency ω_o, $\frac{\text{rad.}}{\text{sec.}}$	6.36	0.73	0.73

FIGURE III THEORETICAL TIME-IMMERSION CURVES

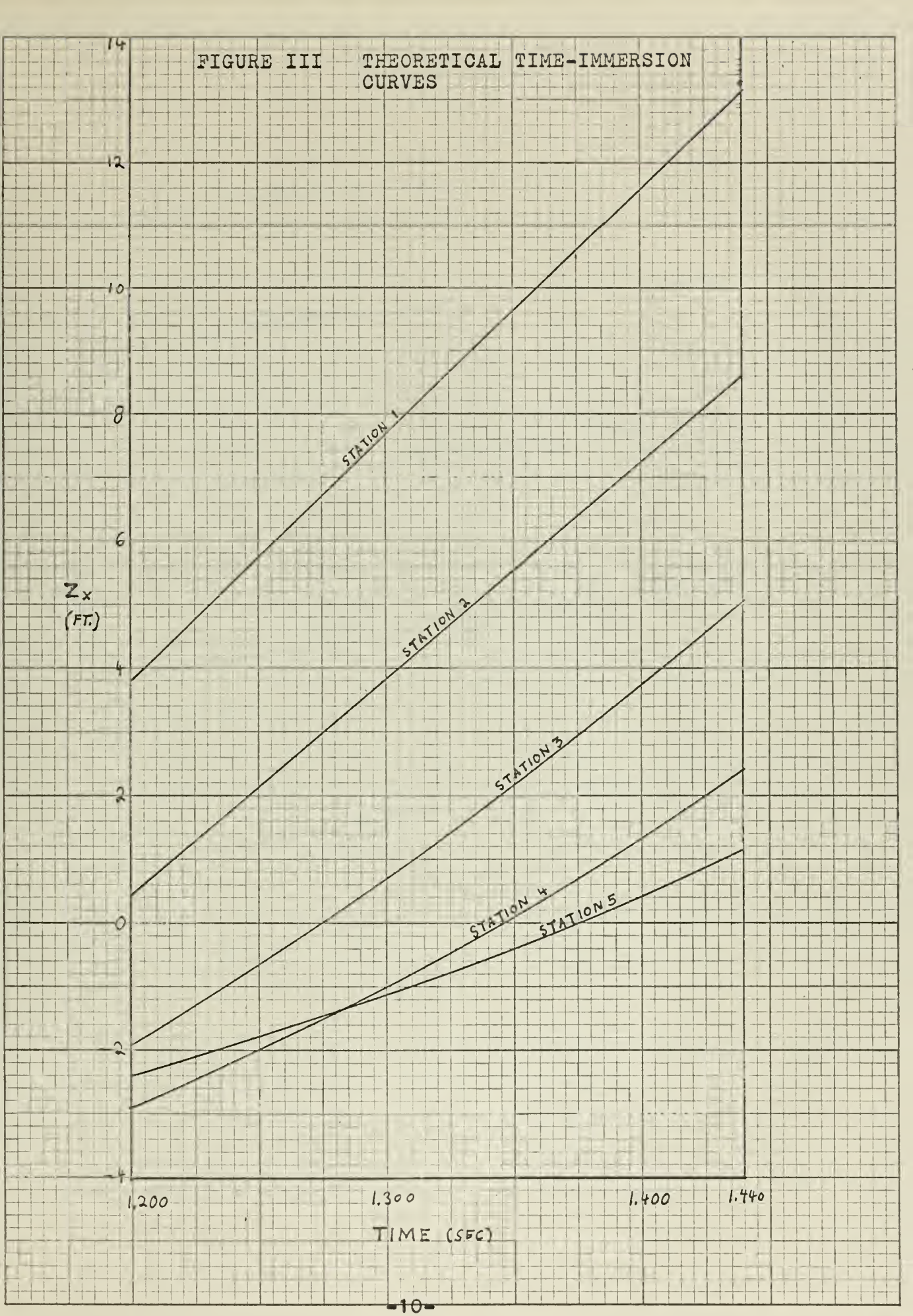

FIGURE IV THEORETICAL TIME-RELATIVE VELOCITY CURVES

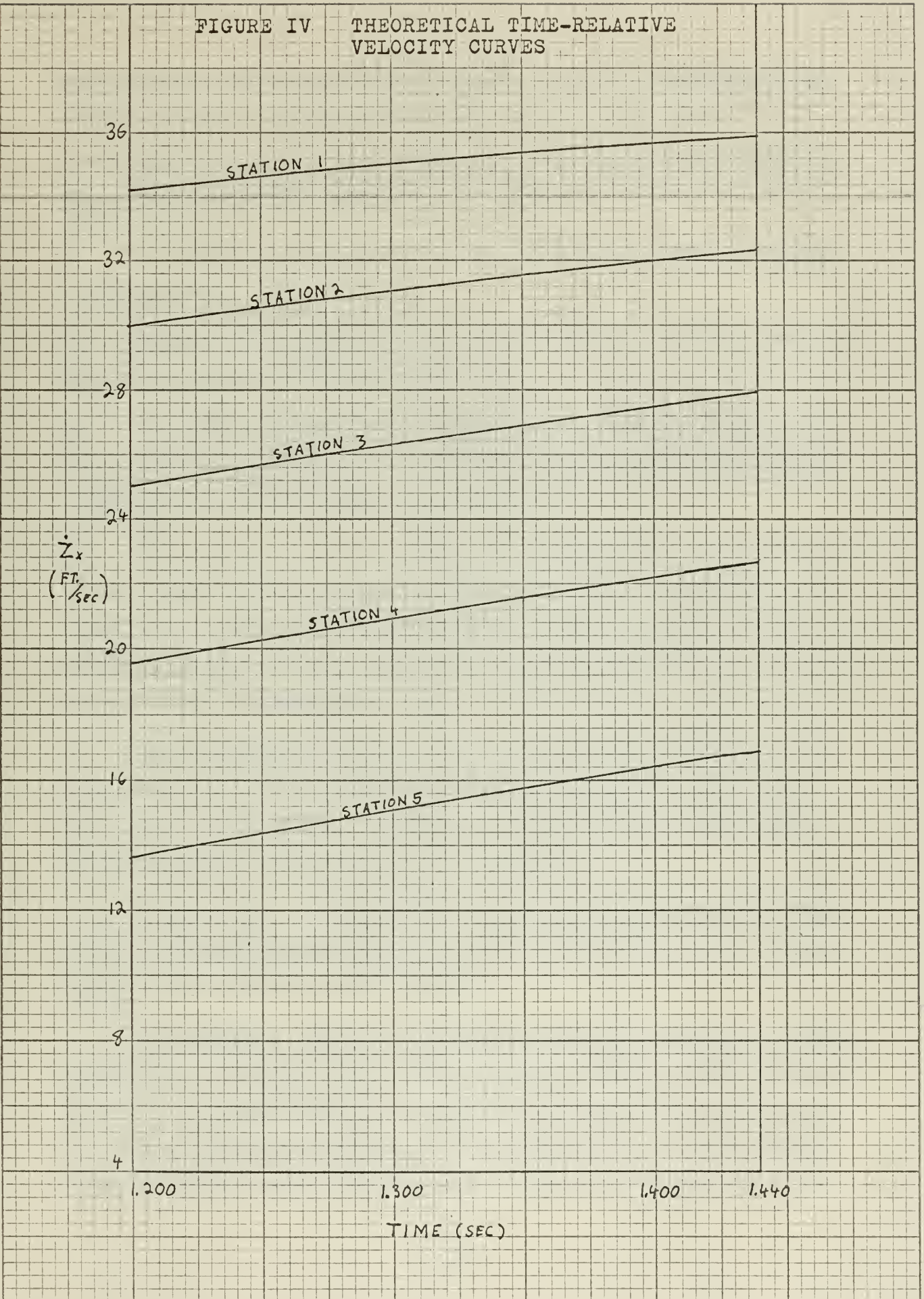

sections (each a station spacing in length), and then combined by strip theory to yield the pressure load on the forefoot of the ship.

2) Each impacting section is assumed to be perfectly rigid and to be symmetrical about the vertical centerline plane.

3) The velocity of penetration is not constant, but varies according to equation (2).

4) The flow field is assumed to be irrotational (a necessary condition for the existence of a velocity potential).

5) The fluid is assumed to be frictionless and incompressible, and the velocity of penetration is assumed to be high enough for the effects of gravity and surface tension to be neglected.

6) On the basis of the assumption of irrotational flow, the particles of the original surface remain on the surface and no new particles are added to the surface (12). Since the fluid is incompressible, the arc length along the surface from the impacting body to any given particle is constant and independent of time.

The preceding conditions do not define the shape of the free surface. However, for a wedge shaped body, which is the mathematical model used for the theory, two general conditions can be formulated which will define the shape of the free surface:

a) Continuity: The fluid displaced by the body must appear above the original water surface in the form of a wave and/or spray. The arc length of the surface must be constant.

b) Similarity: Since the impacting body is symmetrical, and the immersion is normal to the surface, the field of flow is divided into two halves by the centerline of symmetry. By neglecting the gravity forces, the surface shape and dynamic state of the field of flow can be defined entirely in terms of the penetration and velocity of the body (7). If the

sections (each a station spacing in length), and then combined by strip theory to yield the pressure load on the forefoot of the ship.

2) Each impacting section is assumed to be perfectly rigid and to be symmetrical about the vertical centerline plane.

3) The velocity of penetration is not constant, but varies according to equation (9).

4) The flow field is assumed to be irrotational (a necessary condition for the existence of a velocity potential).

5) The fluid is assumed to be frictionless and incompressible, and the velocity of penetration is assumed to be high enough for the effects of gravity and surface tension to be neglected.

6) On the basis of the assumption of irrotational flow, the particles of the original surface remain on the surface and no new particles are added to the surface (12). Since the fluid is incompressible, the arc length along the surface from the impacting body to any given particle is constant and independent of time.

The preceding conditions do not define the shape of the free surface. However, for a wedge shaped body, which is the mathematical model used for the theory, two general conditions can be formulated which will define the shape of the free surface:

a) Continuity: The fluid displaced by the body must appear above the original water surface in the form of a wave and/or spray. The arc length of the surface must be constant.

b) Similarity: Since the impacting body is symmetrical, and the immersion is normal to the surface, the field of flow is divided into two halves by the centerline of symmetry. By neglecting the gravity forces, the surface shape and dynamic state of the field of flow can be defined entirely in terms of the penetration and velocity of the body (V). If the

penetration velocity is constant, the flow field and surface shape must be geometrically and dynamically similar at all times. However, in the present case, the penetration velocity is not constant, and therefore the surface shape is assumed to be only geometrically similar at different times.

Application of General Conditions

CONTINUITY The general shape of the free surface due to penetration by a wedge shaped body is shown in Fig. V. As shown in the figure, the free surface can be thought of as being made up of spray and a wave. The two merge together in the "spray root" area. In determining the free surface shape, the wave rise (η) is given by equations 11 and 13 of reference (13).

$$\eta = \frac{2c \tan\beta}{\pi} \left(\frac{y}{c} \sin^{-1} \frac{c}{y} - 1 \right) \qquad (3)$$

This is the same expression which gives the surface rise in the "expanding plate" theory. The wetted half width (c) is the point on the body which is wetted by the piled up water in the absence of spray. The wetted half width at the original water level is $\frac{2c}{\pi}$ (Wagner; see reference 14). The continuity condition is satisfied if Area A = Area B, and if $s = y$. However, the continuity condition itself is not sufficient to determine the free surface shape since any thickness of spray may be associated with an unlimited variety of waves, and still not violate the continuity requirement. Also, the free surface in the spray root area, where the surface wave and spray merge together, could assume any one of many shapes.

Similarity The principle of similarity for the proportional increase of the wave and spray with continued penetration is the second consideration. Not only must the displaced fluid appear above the original water surface, but the wave and spray must be increasing in such a manner

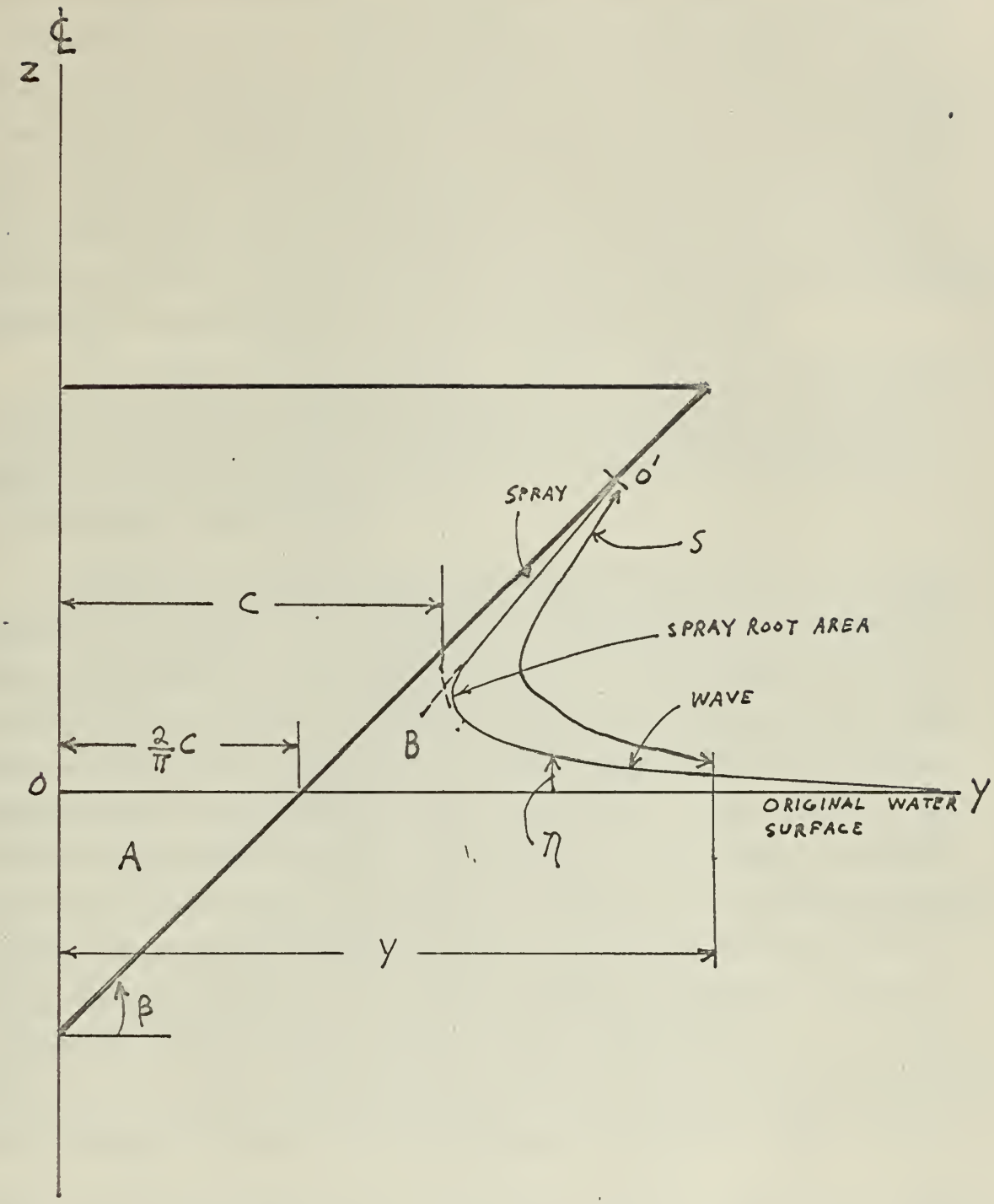

FIGURE V FREE SURFACE DUE TO PENETRATION OF A WEDGE

that the shape and velocities are everywhere determined by the position and penetration velocity of the entering body. By a geometrical construction and integration process proposed by Wagner (see reference 7), it is possible to relate the surface shape and velocities, so that for any spray thickness, one corresponding wave and spray-root shape can be determined which meets the requirements of continuity and similarity. However, Wagner's proposal was for a constant entry velocity, the following theory is developed for a variable penetration velocity.

In an ideal fluid where gravity, viscosity, and surface tension are neglected, the shape of the free surface is uniquely determined by the shape of the impacting body, and the size of the shapes is determined by the amount of penetration .*

Consider the several stages of the penetration process of a wedge shaped body in Figure VI, using an y-z coordinate system. The penetration of the body into the fluid causes the initially flat surface to rise as a wave, and the nearest particles are deflected out along the wedge surface as spray. The resulting surface shape expands as the wedge penetrates deeper. The resulting surface shapes are $o'_1\ a_1\ b_1$, $o'_2\ a_2\ b_2$, etc. For the same relative position in the fluid and on the surface, the pressure and velocity depend upon the surface shape, and must bear the same relationship to the penetration velocity at any instant of time (7). The above statement applies to the relative position in the fluid, and not to a particular fluid particle. The positions are indicated by o'_1, o'_2, o'_3 and a_1, a_2, a_3, etc. If the penetration velocity was constant for the body, the velocity of the fluid at corresponding points would be equal. That is

---

*) Of course this statement is only true for a certain definite time interval after impact. As the body penetrates deeper, much of the free surface shape will be dissipated as spray, and as the penetration velocity decreases, the influence of gravity will be felt.

*) Of course this statement is only true for a certain definite time interval after impact. As the body penetrates deeper, much of the free surface will be displaced as spray, and as the penetration velocity decreases, the influence of gravity will be felt.

$U_{a_1} = U_{a_2} = U_{a_3} = K_a \dot{z}_x$ where K_a represents a proportionality factor between the velocity U at positions a_1, a_2, etc., and the penetration velocity, $\dot{z}_x$. However, for varying velocity, $U_{a_1} \neq U_{a_2} \neq U_{a_3}$, but the velocity at corresponding points will still be proportional to the penetrating velocity.

$$U_{a_1} = K_a \dot{z}_x(t_1), \quad U_{a_2} = K_a \dot{z}_x(t_2)$$
$$U_{b_1} = K_b \dot{z}_x(t_1), \quad U_{b_2} = K_b \dot{z}_x(t_2) \qquad (4)$$

However, it is not unreasonable to assume that $K_{a_1} = K_{a_2} = K_{a_3}$, $K_{b_1} = K_{b_2} = K_{b_3}$, etc. Therefore, the velocity at corresponding points will be directly proportional to the instantaneous penetrating velocity.

The velocity at any point on the free surface, such as a_2 or b_2, is determined from consideration of this condition of similarity. Consider point b_2 for example. A particle on the surface at point b_2 is instantaneously moving along the radius with a velocity U_{rb} and at the same time sliding past the radius toward the spray region with a velocity U_{s_b} (see Fig. VII).

The vector sum of the two motions ($U_{r_b} + U_{s_b}$) yields the instantaneous resultant velocity U_b of the point in question.

The radial expansion velocity, U_r, the velocity of the surface past the radius, U_s, and the resultant velocity, U, are each directly proportional to the penetration velocity, $\dot{z}_x$. Therefore, for constant entry velocity, or for an average velocity taken over a small time interval, the velocity components (U_r, U_s) at a position are constant, and the vector sum may be obtained from the radial distance and the arc length.

Consider the point b_2, on the curve in Figure VI. The radial distance r is given by:

$$\vec{r} = \int_0^t U_{rb}\, dt$$

distance r is given by:

$$\frac{1}{r} = \int_0^{\theta} U^{r\theta}\, d\theta$$

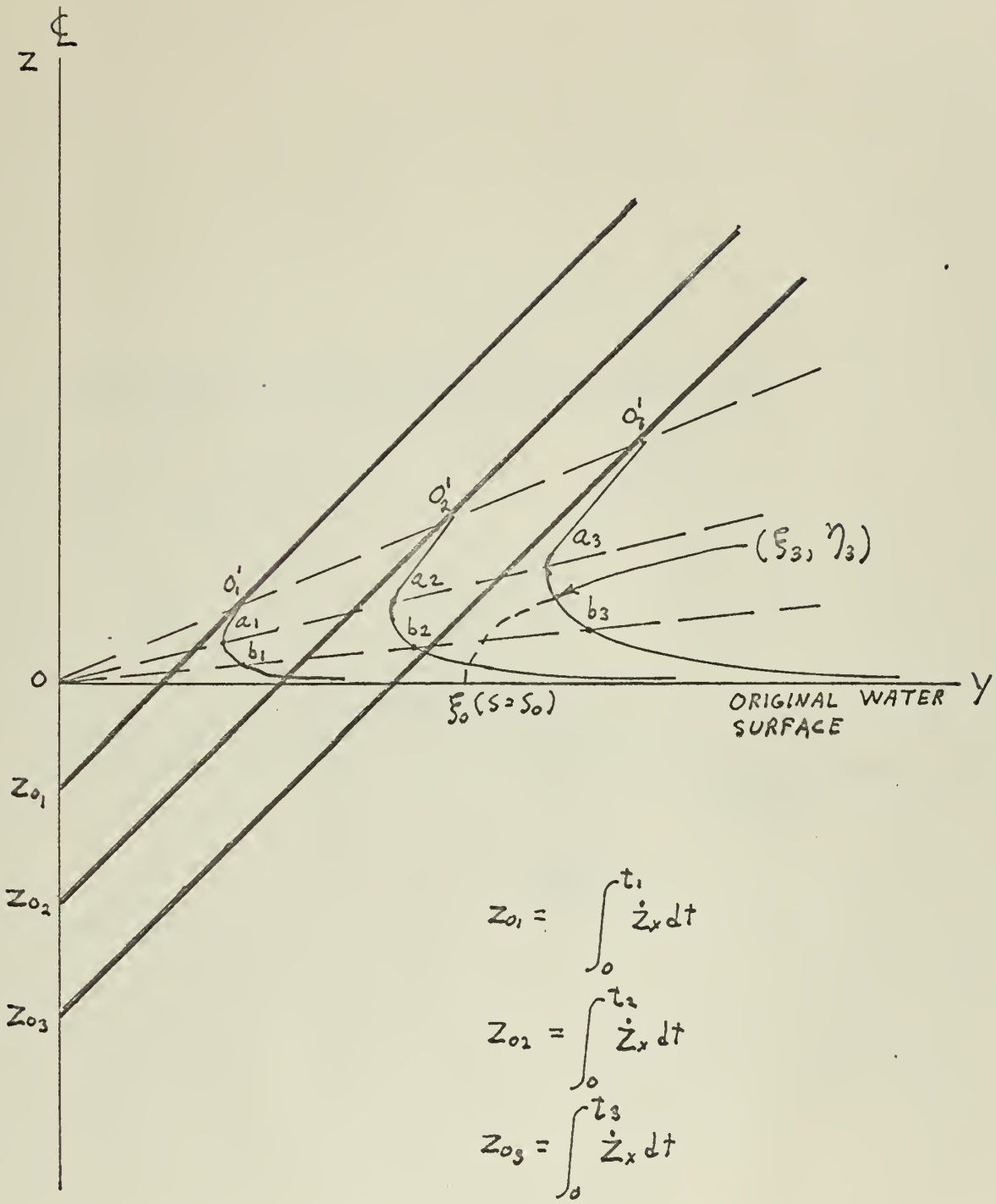

$$Z_{o_1} = \int_o^{t_1} \dot{Z}_x \, dt$$

$$Z_{o_2} = \int_o^{t_2} \dot{Z}_x \, dt$$

$$Z_{o_3} = \int_o^{t_3} \dot{Z}_x \, dt$$

FIGURE VI REPRESENTATION OF SIMILARITY CONDITIONS

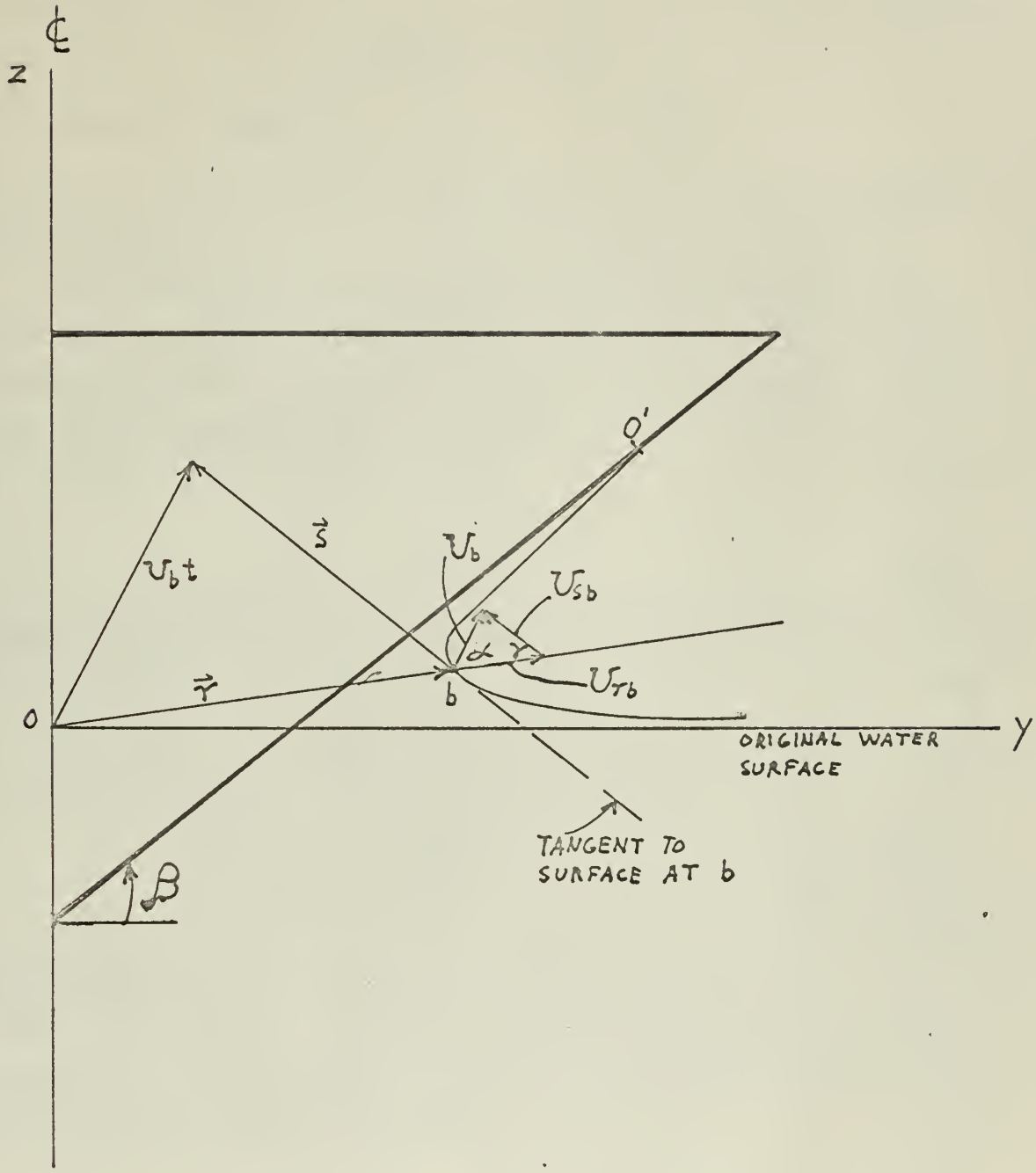

FIGURE VII VELOCITY DIAGRAM

The vector s is constructed tangent to the surface at b_2 so that s equals the arc length $0'b_2$:

$$\vec{s} = \int_0^t U_{sb}\, dt$$

The vector sum is then:

$$\vec{s} + \vec{r} = \int_0^t U_b\, dt \qquad (5)$$

The individual fluid particles do not follow the radiating lines, but remain at a fixed arc length from 0' . The motion of a particle is therefore a function of its relative position on the free surface, and is given by the following integral relations

$$\xi - \xi_o = \int_0^t v\, dt \qquad (6a)$$

$$\eta = \int_0^t w\, dt \qquad (6b)$$

Equations (6) are referred to the y and z axes in Figure VI. The motion in the y direction in a time interval t is expressed by $\xi - \xi_o$, ξ_o being the original position of the particle. The symbol η represents the vertical elevation of a particle (z-direction). Now the velocity of a particle (v, w) is to be determined for any point in its path, so that Equations (6) can be solved. There does not seem to be a simple analytic solution, but a graphical solution can easily be carried out. However, the solution can be simplified by changing the variable of integration from time to arc length. This is done in the following manner. If the penetration velocity was constant, the arc length and times at two corresponding points on the free surface could be related by:

$$\frac{S_{b_2}}{t_2} = U_{sb} = \frac{S_{b_1}}{t_1} = \frac{S_o}{t_1}$$

(reference (7)). However, for varying velocity at time t, $U_{sb} = K_{sb}\, \dot{z}_x(t_1)$, where K_{sb} is the proportionality factor which relates the velocity of the

The vector e is constructed tangent to the surface at P_1 so that e equals the arc length $0'P_1$:

$$\vec{e} = \int_0^{t_1} \vec{v}^{ab}\, dt$$

The vector sum is then:

$$\vec{s} = \vec{r} + \int_0^{t_c} \vec{v}^{b}\, dt \qquad (3)$$

The individual fluid particles do not follow the vaulting lines, but remain on a fixed arc length from $0'$. The motion of a particle is therefore a function of its velocity position on the free surface, and is given by the following integral relations

$$\xi - \xi_0 = \int_0^{t} u\, dt \qquad (3a)$$

$$\eta = \int_0^{t} v\, dt \qquad (3b)$$

Equations (3) are referred to the y and z axes in Figure VI. The motion in the y direction in a time interval t is expressed by $\xi - \xi_0$, being the original position of the particle. The symbol η represents the vertical elevation of a particle (z-direction). Here the velocity of a particle (v, w) is to be determined for any point in its path. In that figuration (3) can be solved. There does not seem to be a simple analytic solution, but a graphical solution can readily be carried out. However, the solution can be simplified by changing the variable of integration from time to arc length. This is done in the following manner. If the penetration velocity was constant, the arc length and time at the corresponding points on the free surface could be related by:

$$\frac{s_{ab}}{t} = v^{ab} = \frac{v_{ab}}{c} \cdot \frac{s_c}{t}$$

(reference (7)). However, for varying velocity at time t, $v^{ab} = K^{ab}\, \dot{s}^{b}(t)$, where K^{ab} is the proportionality factor which relates the velocity of the

surface sliding past the radius 0b to penetration velocity. However, in the time interval from t_1 to t_2, we can assume that U_{sb} is constant and equal to its average value. According to reference (15), an average valve for a function, f(t), can be defined as follows:

$$\mu f(t) = \frac{1}{2}\left[f\left(t + \frac{\Delta t}{2}\right) + f\left(t - \frac{\Delta t}{2}\right)\right]$$

Therefore, at time $\frac{t_1 + t_2}{2}$, the average value of U_{sb} can be assumed to be constant over the interval t_1 to t_2. For any time, t_2,

$$\frac{S_{b_2}}{t_2} = U_{sb}\left(\frac{t_1 + t_2}{2}\right) = \frac{S_o}{t}$$

By this reasoning, an expression for arc length in terms of time can be obtained for any time interval, Δt:

$$t = \frac{S_o t_2}{S}$$

where t = the earlier time, and S = corresponding arc length on the surface at time t_2.

Also, $$dt = -\frac{S_o t_2}{S^2}\, ds$$

Substitution for dt in Equations (6a) and (6b) yields

$$\xi - \xi_o = \int_{\infty}^{S_o} v\left(-\frac{S_o t_2}{S^2}\, ds\right) = S_o \int_{S_o}^{\infty} \frac{v t_2}{S^2}\, ds \qquad (7a)$$

$$\eta = S_o \int_{S_o}^{\infty} \frac{w t_2}{S^2}\, ds \qquad (7b)$$

Equations (7a) and (7b) can be solved numerically as follows:

Referring to Fig. VI, it is seen that the penetration velocity has approximately a linear variation over the time interval under consideration. Since the particle velocities at corresponding points are directly proportional to the penetration velocity, they can also be assumed to vary linearly. Using this assumption, the integral in Equation (5) can be expressed as

surface sliding past the radius R_o to penetration velocity. However, in the time interval from t_1 to t_2, we can assume that U_{ab} is constant and equal to its average value. According to reference (16), an average value for a function, $f(t)$, can be defined as follows:

$$\mu f(t) = \frac{1}{2}\left[f\left(t+\frac{\Delta t}{2}\right) + f\left(t - \frac{\Delta t}{2}\right)\right]$$

Therefore, at time $\frac{t_1 + t_2}{2}$, the average value of U_{ab} can be assumed to be constant over the interval t_1 to t_2. For any time, t_2,

$$\frac{S_2}{t_2} = U_{ab}\left(\frac{t_1 + t_2}{2}\right) = \frac{S_o}{t}$$

By this reasoning, an expression for arc length in terms of time can be obtained for any time interval, Δt:

$$t = \frac{S_o t_2}{S}$$

where t = the earlier time, and S = corresponding arc length on the surface at time t_2.

Also, $$dt = -\frac{S_o t_2}{S^2}\, ds$$

Substitution for dt in Equations (6a) and (6b) yields

$$\xi - \xi_o = \int_{\infty}^{S_o} v\left(-\frac{S_o t_2}{S^2}\, ds\right) = S_o \int_{S_o}^{\infty} \frac{v t_2}{S^2}\, ds \qquad (7a)$$

$$\eta = S_o \int_{S_o}^{\infty} \frac{w t_2}{S^2}\, ds \qquad (7b)$$

Equations (7a) and (7b) can be solved numerically as follows:

Referring to Fig. VI, it is seen that the penetration velocity has approximately a linear variation over the time interval under consideration. Since the particle velocities at corresponding points are directly proportional to the penetration velocity, they can also be assumed to vary linearly. Using this assumption, the integral in Equation (6) can be expressed as

$$\vec{S} + \vec{r} = \int_o^t U_b \, dt = U_b t \qquad (5)$$

where U_b is the average value of U_b for the time interval under question. From this, the average value of the velocity components, in Equations (7a) and (7b) can be found (vt and wt). Therefore, a step by step integration of Equations (7a) and (7b) can be carried out as shown in Appendix A. Any trial free surface shape which satisfies continuity can be used for the determination of the surface velocities. The velocities are then used to determine a new surface shape. This procedure is carried out until there is a negligible difference between assumed and computed values of surface shape.

The integral equations (7a) and (7b) relate the surface rise at a point to all the points more distant from the body. Therefore, the path of each particle on the surface follows the same related path, and the conditions for similarity are satisfied. It would appear that the integral equations reduce the number of spray-wave combinations to one for each spray thickness (7).

The spray root thickness itself was shown in reference (7) to be related to wetted width (c) and deadrise angle (β):

$$\delta = c \left(\frac{\beta}{\pi} \right)^2 \qquad (8)$$

Potential on Free Surface

Referring to Figure VII, the tangential velocity, $\frac{\partial \Phi}{\partial S}$ along the surface at a position, b is given by $- U_{sb} + U_{rb} \cos \gamma$. For points along the surface (at a specific depth) $\cos \gamma = \frac{dr}{ds}$ *.

Therefore,

$$- \frac{\partial \Phi}{\partial s} = U_{sb} - U_{rb} \cos \gamma = U_{sb} - U_{rb} \frac{dr}{ds} \qquad (9)$$

*) $\frac{dr}{ds}$ for a particular surface should not be confused with $\frac{dr}{ds} = r/s$ for a constant position, such as b.

*) $\frac{dz}{da}$ constant position, such as b.

Since U_{sb} and U_{rb} are proportional to $\dot{z}_x$, and $\dot{z}_x$ can be assumed equal to a mean value over the time interval under consideration, U_s and U_r can be considered approximately constant over the same time interval. A differential equation can be obtained by multiplying Equation (9) by tds. ($tU_s \approx s$, $t\,U_r \approx r$):

$$-td\phi = sds - rdr$$

Integration yields

$$-t\phi = \frac{(s^2 - r^2)}{2} + A \qquad (10)$$

Since $\phi = 0$ at $s = r = \infty$, $A = 0$, and $\phi = \frac{r^2 - s^2}{2t}$ (11)

which is an approximate expression for the velocity potential on the free surface with varying penetration velocity.

Potential and Velocity Distributions on Body Surface

Assuming that the free surface shape for a given deadrise angle is unique, and is a result of potential flow, the velocity and potential at any point can be represented by a complex analytic function:

$$U = \frac{dw}{dz} = v - iv, \qquad w = \phi + i\psi$$

The Cauchy integral equation may be applied to the complex function as described in reference (7). By Cauchy's integral formula, a value of an analytic function in a region is determined by its values on the boundary. There is no choice of ways in which the function can be defined at points away from the boundary once the function is defined on the boundary. Every change of values of the function at interior points must be accompanied by a change of its values on the boundary if the function is to remain analytic (16). The integral formula for the point within the boundary is:

$$f(z_o) = \frac{1}{2\pi i} \int_C \frac{f(z)}{z - z_o}\, dz \qquad (12)$$

z is the complex coordinate of the position in the field. Since points on the solid boundary are being investigated, the bounding contour circles only halfway around the point so that $2\pi i$ becomes πi. Also, $f(z) = u + iv = U(z)$ on the boundary, and equation (12) becomes:

$$U(z_o) = \frac{1}{\pi i}\int_C \frac{U(z)}{z-z_o}\,dz \qquad (13)$$

The expression can be separated into the real and imaginary parts by placing the origin of coordinates at the point z_o under consideration, and writing z in the polar form:

$$z = Re^{i\theta} = e^{\ln R + i\theta} \qquad (14)$$

$$dz = e^{\ln R + i\theta}\left[d(\ln R) + id\theta\right] \qquad (15)$$

Substitution of the expression for z and dz into Equation (13) yields

$$U(z_o) = U_o - iv_o = \frac{1}{\pi i}\int_C U - iv\left[d(\ln R) + id\theta\right] \qquad (16)$$

Rearranging terms gives

$$i\pi U + \pi v = \int_C d(\ln R) + vd\theta + i\left[Ud\theta - vd(\ln R)\right],$$

so that the real and imaginary parts may be separated:

$$v_o = \frac{1}{\pi}\int vd\theta + Ud(\ln R) \qquad (17a)$$

$$U_o = \frac{1}{\pi}\int d\theta - vd(\ln R) \qquad (17b)$$

The construction for performing the numerical integration of the above equations is shown in Figure VIII. The complex coordinates were oriented so that the y-axis (imaginary axis) is along the wedge, positive toward the spray tip. The x-axis (real axis) is normal to the body and positive out. The potential on the body surface may be obtained by integrating the velocity along the wedge from the spray tip to the apex.

Pressure Distribution

The general equation for fluid pressure in a potential flow of in-

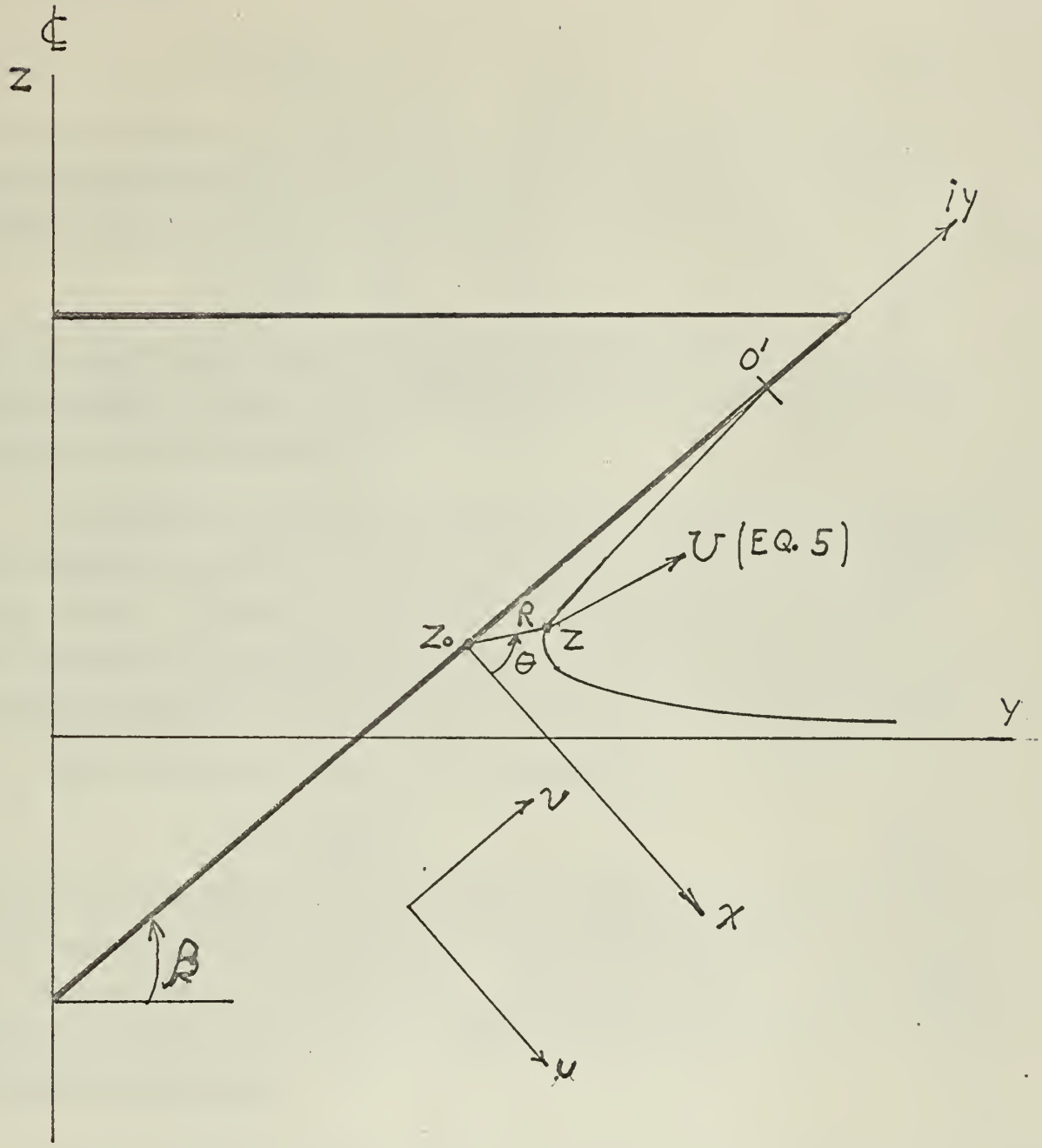

FIGURE VIII POLAR COORDINATE SYSTEM FOR THE DETERMINATION OF THE VELOCITY POTENTIAL ALONG THE BODY SURFACE

compressible fluid, is used to determine the pressure distribution on the body (12)

$$\frac{p}{\rho} = \frac{\partial \Phi}{\partial t} - \Omega - \frac{U^2}{2} + F(t) \qquad (18)$$

The gravity force (Ω) and extraneous impulses ($F(t)$) are zero since gravity has been neglected, and the fluid was assumed to be at rest at infinity. Therefore Equation (18) becomes

$$\frac{p}{\rho} = \frac{\partial \Phi}{\partial t} - \frac{U^2}{2} \qquad (19)$$

The resultant field velocity (U) can be determined on the free surface (Equation (5)), and on the body (Equation (17)). Now it remains to determine an expression for $\frac{\partial \Psi}{\partial t}$.

Assume that the depth of penetration at time t_1 is given by the average penetration velocity ($\dot{z}_x$), in the interval $t = o$ to $t = t_1$, multiplied by t_1. This is the same as assuming constant velocity penetration in the specified time interval. At any position, (r_t, z_o) * in the fluid, the potential is therefore a linear function of time in the interval to t_1 (7).

For any time interval t_2 to t, assuming $\overline{\dot{z}}_x$,

$$\Phi r_t = \Phi r_{t_2} \frac{t}{t_1} \qquad (20)$$

However, for a fixed point (y, z) in the flow field, the above expression is not correct. If the point (y, z) coincides with the position r_{t_1}, z_o at t_1, at time $t = t_1 + \Delta t$ the position $r_{t_1+\Delta t}$, z_o is a distance $\Delta r = \frac{r \Delta t}{t}$ from (y, z). For small Δt, the resultant vector velocity can be assumed constant in the region.

At $t = t_2$ $\Phi(y, z) = \Phi_{r_{t_1}}$ and at $t = t_1 + \Delta t$ $\Phi(y, z)_{t_1+\Delta t} = \Phi_{r_t} - U\cos a(\Delta r)$

---

*) See Figure IX, (r_t, z_o) refers to the distance to the same relative point in the fluid at a depth of penetration z_o. Therefore, as time increases, r_t increases.

compressible fluid, is used to determine the pressure distribution on the body (12)

$$\frac{p}{\rho} = -\frac{\partial\phi}{\partial t} - \Omega - \frac{U^2}{2} + F(t) \qquad (18)$$

The gravity force (Ω) and extraneous impulses (F(t)) are zero since gravity has been neglected, and the fluid was assumed to be at rest at infinity. Therefore Equation (18) becomes

$$\frac{p}{\rho} = -\frac{\partial\phi}{\partial t} - \frac{U^2}{2} \qquad (19)$$

The resultant field velocity (U) can be determined on the free surface (Equation (6)), and on the body (Equation (17)). Now it remains to determine an expression for $\frac{\partial\phi}{\partial t}$.

Assume that the depth of penetration at time t_1 is given by the average penetration velocity ($\bar{\dot{z}}_s$), in the interval t = 0 to t = t_1, multiplied by t_1. This is the same as assuming constant velocity penetration in the specified time interval. At any position, (r_t, z_s)* in the field, the potential is therefore a linear function of time in the interval to t_1 (7).

For any time interval t_0 to t_1 assuming $\bar{\dot{z}}_s$,

$$\phi r_t = \phi r_{t_1} \frac{t}{t_1} \qquad (20)$$

However, for a fixed point (r, z) in the flow field, the above expression is not correct. If the point (r, z) coincides with the position r_{t_1}, z_{t_1} at t_1, at time $t = t_1 + \Delta t$ the position $r_{t_1+\Delta t}$, z_s is a distance $\Delta r = \frac{r\,\Delta t}{t}$ from (r, z). For small Δt, the resultant vector velocity can be assumed constant in the region.

At $t = t_1$ $\phi(r, z) = \phi r_{t_1}$ and at $t = t_1 + \Delta t$ $\phi(r, z)_{t_1+\Delta t} = \phi_{r_1}$ − [illegible]

---

*) See Figure IX. (r_t, z_s) refers to the distance to the same relative point in the field at a depth of penetration z_s. Therefore, as time increases, r_t increases.

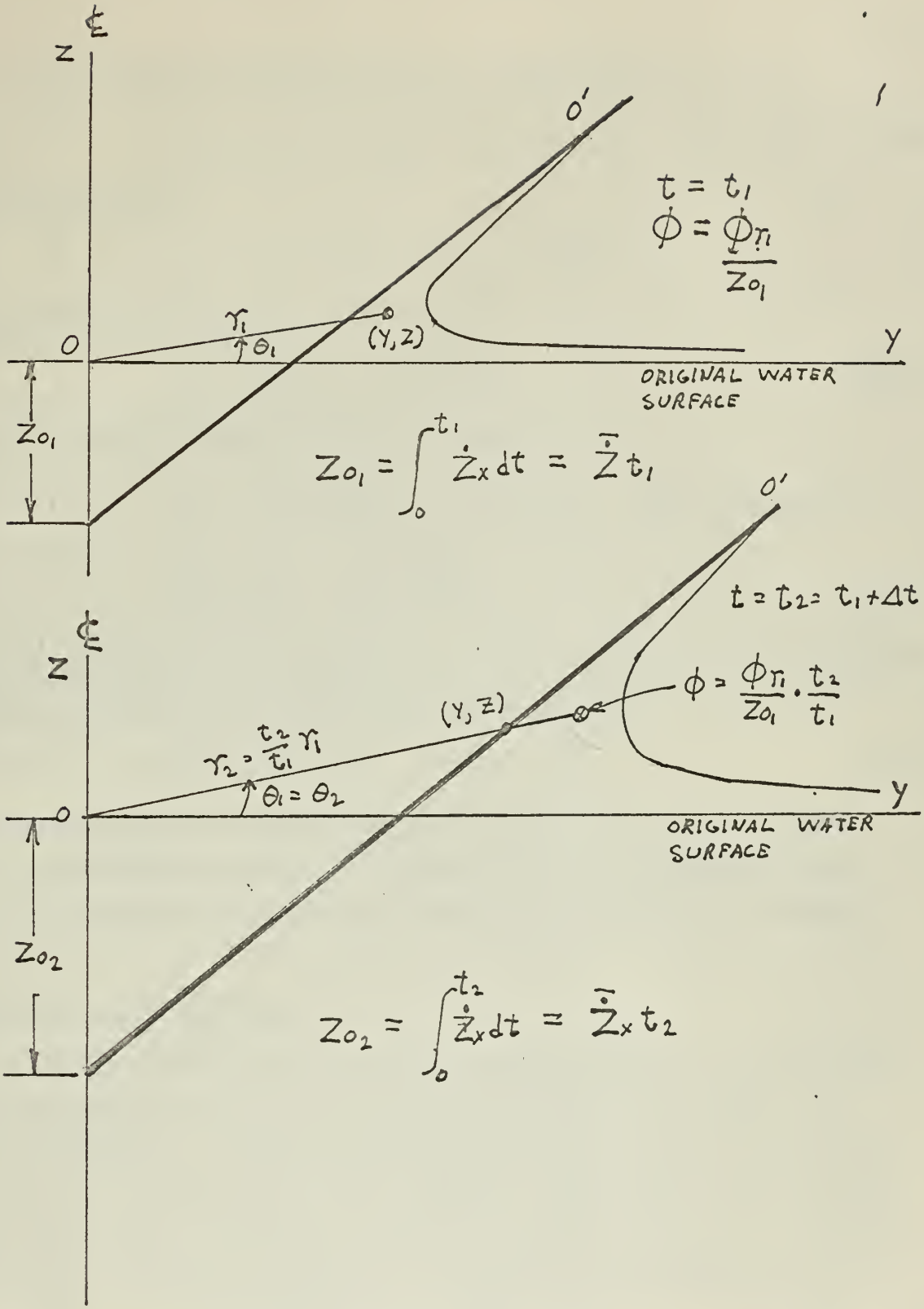

FIGURE IX FIXED AND RELATIVE POSITION POINTS IN THE FLUID

U cos α is the velocity component along . Therefore,

$$\Delta\phi = \phi(y, z)_{t_1+\Delta t} - \phi(y, z)_{t_1} = \phi_t - U\Delta r \cos\alpha - \phi_{r_{t_1}} \quad (21)$$

From Equation (20)

$$\phi_{r_t} = \phi_{r_{t_1}} \frac{t_1 + \Delta t}{t_1} = \phi_{r_{t_1}} + \frac{\Delta t}{t_1} \phi_{r_{t_1}}$$

Equation (21) then becomes

$$\Delta\phi = \frac{\Delta t}{t_1} \phi_{r_{t_1}} - U\Delta t \cos\alpha \quad (22)$$

Taking the limit of Equation (22) as Δt approaches 0:

$$\frac{\partial\phi}{\partial t} = \lim_{\Delta t \to 0} \frac{\Delta\phi}{\Delta t} = \lim_{\Delta t \to 0} \left(\frac{\phi_{r_{t_1}}}{t_1} - \frac{\Delta r}{\Delta t} U \cos\alpha \right)$$

$$\frac{\partial\phi}{\partial t} = \frac{\phi}{t} - \frac{r}{t} U \cos\alpha \quad (23)$$

Equation (23) now applies to all points in the fluid. The pressure distribution is given by substituting Equation (23) in Equation (19).

$$\frac{p}{\rho} = -\frac{\phi}{t} + \frac{r}{t} U \cos\alpha - \frac{U^2}{2} \quad (24)$$

On the body surface, the pressure may be found by using the values of , ϕ, U, and α already determined. The total load on the body is obtained from the integration of the pressure across the projected wetted width.

Application to Ship Sections

There are two possible methods of solving the water entry problem of bodies of general shape by considering the free surface shape. The first is to construct the free surface based on the boundary of the actual ship section as it enters the water. However, this method is questionable since the similarity principle has not been proved to hold for a body of general shape. The second method is to approximate the ship section by a wedge-like shape of an equivalent deadrise angle.

The period of interest in a slamming investigation, for a certain

U cos a is the velocity component along . Therefore,

$$\Delta\phi = \phi(\xi, \eta)\Big|_{t_1+\Delta t} - \phi(\xi, \eta)\Big|_{t_1} = \phi_{\gamma_2} - U\Delta\gamma \cos a - \phi_{\gamma_1} \qquad (21)$$

From Equation (16)

$$\phi_{\gamma_2} = \phi_{\gamma_1}\frac{t_1 + dt}{t_1} = \phi_{\gamma_1} + \phi_{\gamma_1}\frac{\Delta t}{t_1}$$

Equation (21) then becomes

$$\Delta\phi = \frac{\Delta t}{t_1}\phi_{\gamma_1} - U\Delta t \cos a \qquad (22)$$

Taking the limit of Equation (22) as Δt approaches 0:

$$\frac{\partial\phi}{\partial t} = \lim_{\Delta t \to 0}\frac{\Delta\phi}{\Delta t} = \lim_{\Delta t \to 0}\left(\frac{\phi_{\gamma_1}}{t_1} - \frac{\Delta\gamma}{\Delta t}\, U \cos a\right)$$

$$\frac{\partial\phi}{\partial t} = \frac{\phi}{t} - \frac{\gamma}{t}\, U \cos a \qquad (23)$$

Equation (23) now applies to all points in the fluid. The pressure distribution is given by substituting Equation (23) in Equation (14).

$$\frac{p}{\rho} = -\frac{\phi}{t} + \frac{\gamma}{t}\, U \cos a - \frac{q^2}{2} \qquad (24)$$

On the body surface, the pressure may be found by using the values of ϕ, U, and a already determined. The total load on the body is obtained from the integration of the pressure across the projected wetted width.

Application to Ship Sections

There are two possible methods of solving the water entry problem of bodies of general shape by considering the free surface shape. The first is to construct the free surface based on the boundary of the actual ship section as it enters the water. However, this method is questionable since the similarity principle has not been proved to hold for a body of general shape. The second method is to approximate the ship section by a wedge-like shape of an equivalent deadrise angle.

The period of interest in a slamming investigation, for a certain

ship section, is the time period immediately after impact with the water. The maximum impact force is produced either at the instant of impact, or immediately after entry. For the Liberty ship investigated in reference (3), it was found that the slamming pressures were of little significance by the time the draft at station 5 was 9.2 ft. In fact, the time interval of significant pressures was less than 0.17 sec. For this problem, the time interval under investigation is 0.24 sec.

For a hull section with sharp curvature, the spray will not necessarily adhere to the boundary. From photographs of wedge impacts in references (14, 17), the spray, after it leaves the wedge surface, shoots off at an angle roughly equivalent to the deadrise angle (see Fig. X). Therefore, it seems possible that V-shaped sections, or sections with fine lines, could be approximated by a wedge of a certain deadrise angle. However, slamming is more dangerous for sections with small deadrise angles. It is obvious that these sections could not satisfactorily be represented by a V-shaped wedge.

For U-shaped sections with small deadrise angles, the method for constructing the free surface shape will have to be modified. It is obvious that the wave rise cannot be estimated correctly by Equation (3). Figure XI is a sketch of a typical U-shaped section. The pressure distribution for such a section is satisfactorily predicted by the expanding plate theory, except in the spray root region, from $y = b$ to $y = c$. It is therefore reasonable to expect that the pressure on the flat portion of the hull can be given by assuming the pressure distribution for a flat plate from $y = 0$ to $y = b$. The flow past this "flat plate" can be used to estimate the wave height at the free surface. From (18) the distribution of the normal velocity for a flat plate of width $2a$, at points $y > a$, is given by

$$V_n = \frac{V_\infty}{\sqrt{1 - \frac{a^2}{y^2}}} = \frac{\dot{z}_x}{\sqrt{1 - \frac{a^2}{y^2}}} \qquad (25)$$

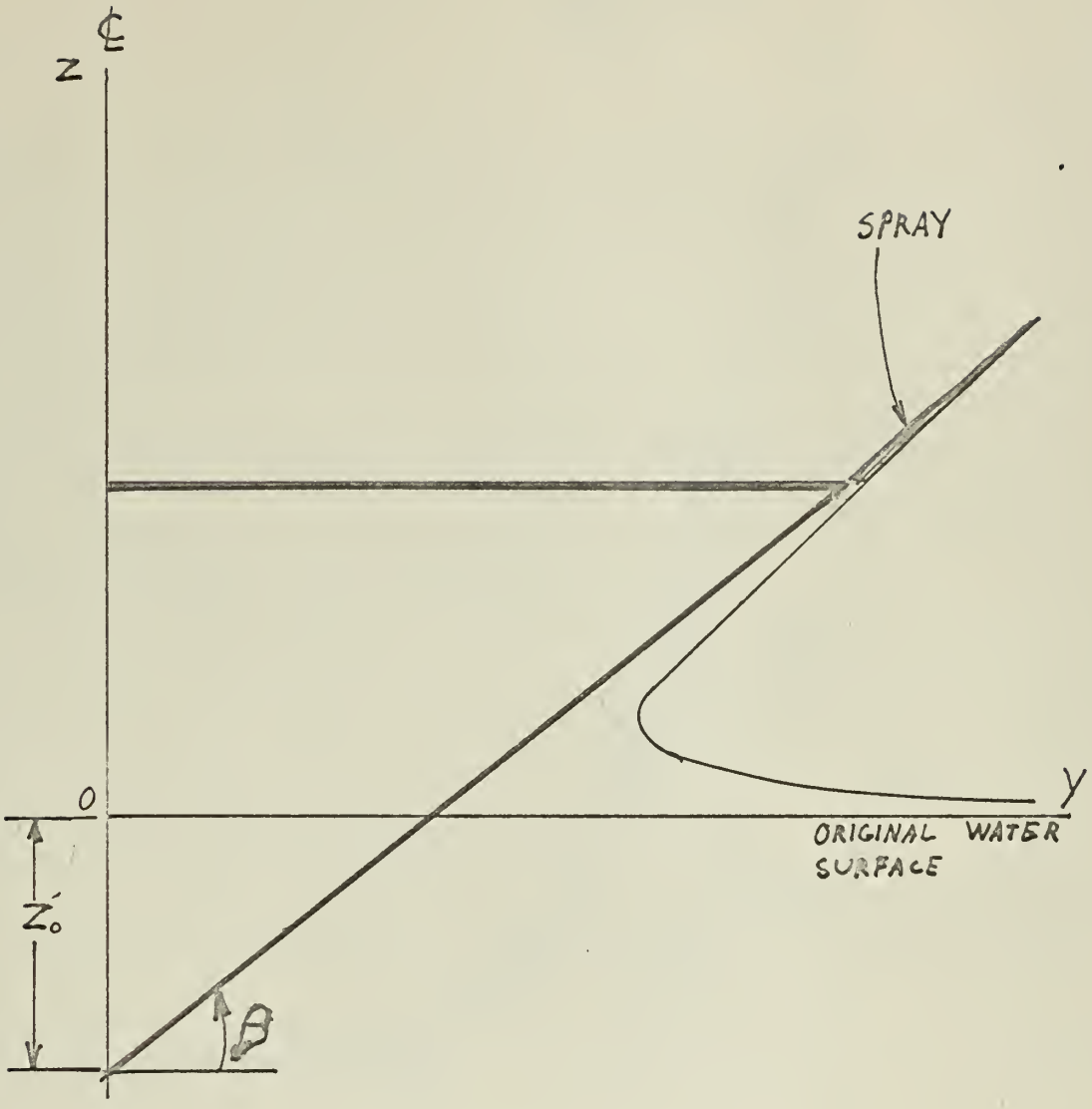

FIGURE X IMPACTING WEDGE

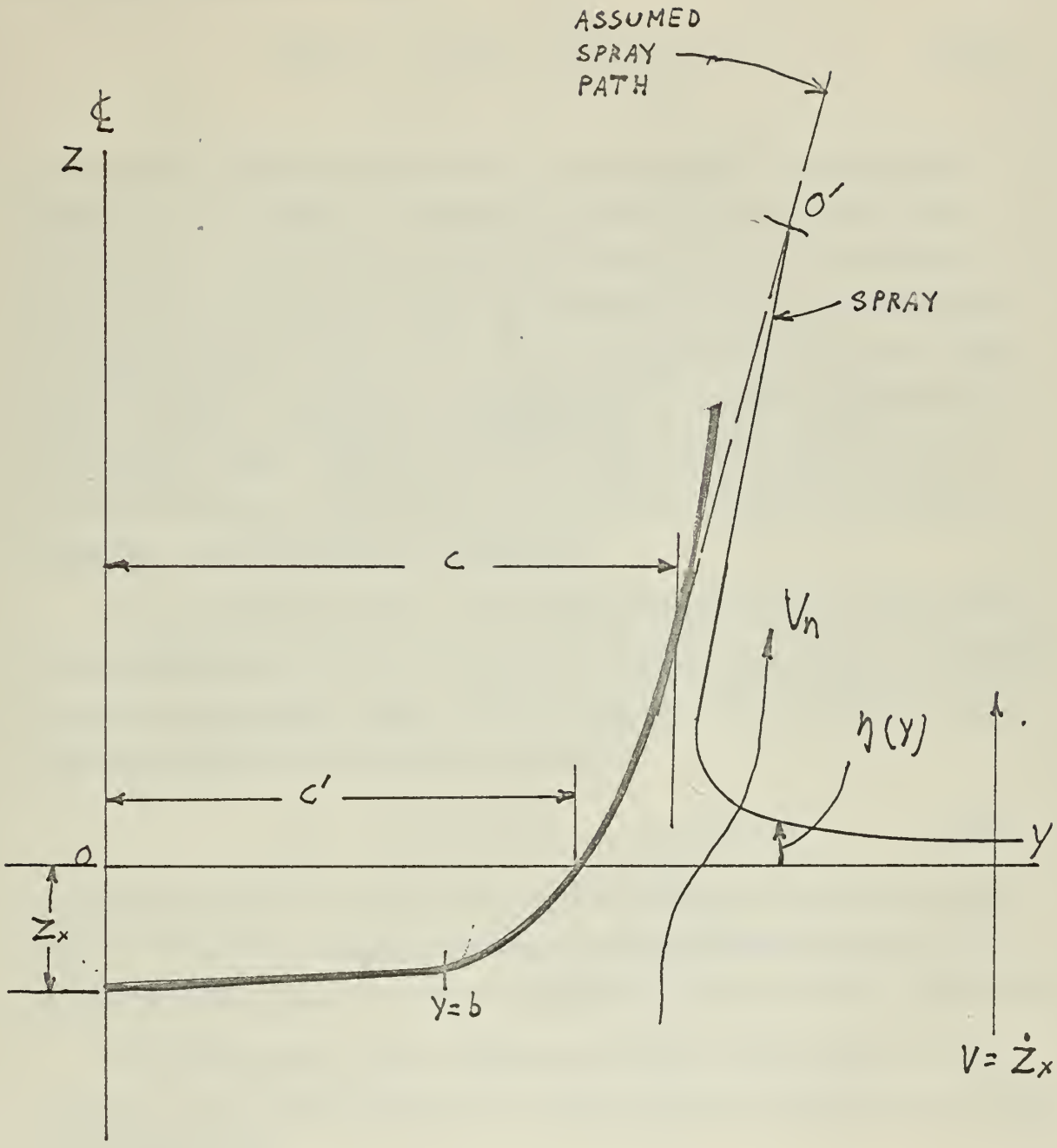

FIGURE XI FLOW NOMENCLATURE

V_n will be the velocity of the free surface particles. The wave height at a point y can be found by:

$$\eta(y) = \int_o^t V_n \, dt = \int_o^t \frac{\dot{z}_x}{\sqrt{1 - \frac{a^2}{y^2}}} dt \qquad (27)$$

For the wave height determinations, the dimension a is taken to be equal to c', the width of the section immersed at the original water line (see Fig. XI). When constructing the free surface, the spray is assumed to shoot off at an angle determined by the slope of the hull in the spray root area. This is the same as assuming that the side of the ship is straight, and that the impacting body is roughly equivalent to a blunt nosed wedge. Assuming that the similarity principle still holds, the free surface is constructed by using the arc length and continuity conditions, and checking by Equation (6).

For a U-shaped section, the velocity potential for the flat portion of the hull (from y = 0 to y = b) can be assumed to be that for irrotational flow about a flat plate. From (19) the complex velocity potential past a plate perpendicular to the flow is given by:

$$\phi = -iv\sqrt{y^2 - a^2} = -\dot{z}_x\sqrt{a^2 - y^2} \qquad (28)$$

Equation (17) can be used to compute the velocity potential on the hull from y = b to y = c. The two velocity potentials should agree at y = b for any specific time. (A sample calculation is discussed in Appendix A.)

The calculations, from which the results in this paper were determined, were carried out for the Lewis type ship discussed previously (see Figure XII).

V^n will be the velocity of the free surface particles. The wave height at a point y can be found by:

$$\eta(y) = \int_0^t V^n \, dt = \int_0^t \frac{x^n}{\sqrt{1 - \frac{y^2}{a^2}}} \, dt \qquad (37)$$

For the wave height determinations, the dimension a is taken to be equal to a', the width of the section immersed at the original water line (see Fig. 22). When constructing the free surface, the spray is assumed to shoot off at an angle determined by the slope of the hull in the spray root area. This is the same as assuming that the side of the ship is straight, and that the impacting body is roughly equivalent to a blunt nosed wedge. Assuming that the similarity principle still holds, the free surface is constructed by using the arc length and continuity conditions, and checking by Equation (9).

For a U-shaped section, the velocity potential for the flat portion of the hull (from $y = 0$ to $y = b$) can be assumed to be that for two-dimensional flow about a flat plate. From (12) the complex velocity potential past a plate perpendicular to the flow is given by:

$$\phi = -(x\sqrt{y^2 - a^2} - \dot{x}^n\sqrt{a'^2 - y^2}) \qquad (38)$$

Equation (17) can be used to compute the velocity potential on the hull from $y = b$ to $y = c$. The two velocity potentials should agree at $y = b$ for any specific time. (A sample calculation is discussed in Appendix A.)

The calculations, from which the results in this paper were determined, were carried out for the Lewis type ship discussed previously (see Figure XII).

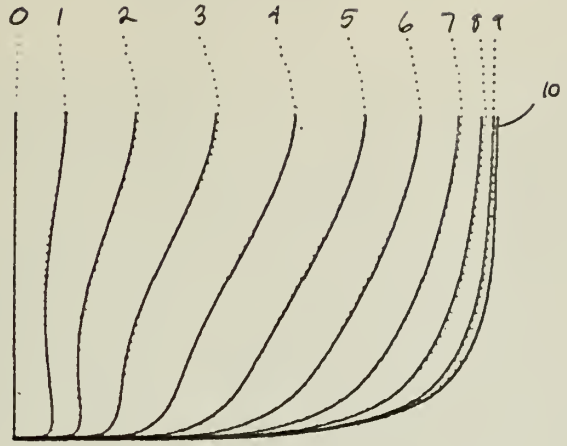

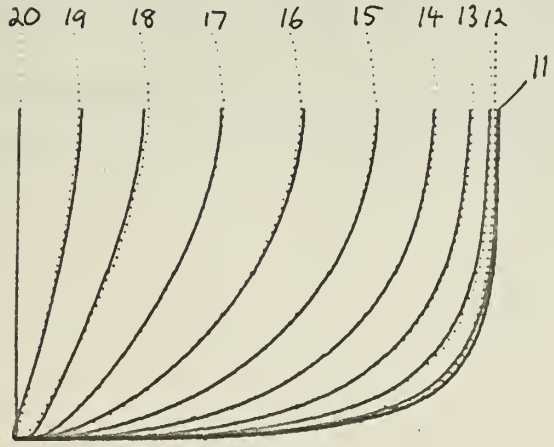

FIGURE XII LEWIS SECTION SHAPES

III. RESULTS

Included in this section are the curves of the theoretical pressure distribution for the ship under consideration. These curves are shown in Figures XIII - XV . Also, one transverse section of the Liberty ship, used as a model in reference (3), was investigated. The pressure distribution for this section is shown in Figure XVII. This section was quite V-shaped and had a deadrise angle of $\beta = 30°$. Straight wedge theory was used for calculation of the pressure distribution, and the results are compared with the results given in reference (3) for the same section.

A sample calculation for station 3 of the Lewis section ship is discussed in Appendix A. The tangential velocity (v_o) on the flat portion of the hull was calculated by two methods (Table IV). The first method was by the assumption of flow over a flat plate. This is the method used for all of the low deadrise sections under consideration. However, for comparison, the tangential velocity on the bottom of the hull was calculated by use of the Cauchy integral formula and equation (17). The results check closely with those from the flat plate flow assumption.

The pressures load on the forefoot was determined by strip theory for several instants of time. The integrated load distribution is shown in Figure XVI.

III. RESULTS

FIGURE XIII PRESSURE DISTRIBUTION ON FOREFOOT OF LEWIS SECTION SHIP AT TIME = 1.284 SEC.

STATION	DRAFT, FT.
1	7.0
2	3.1
3	0.3

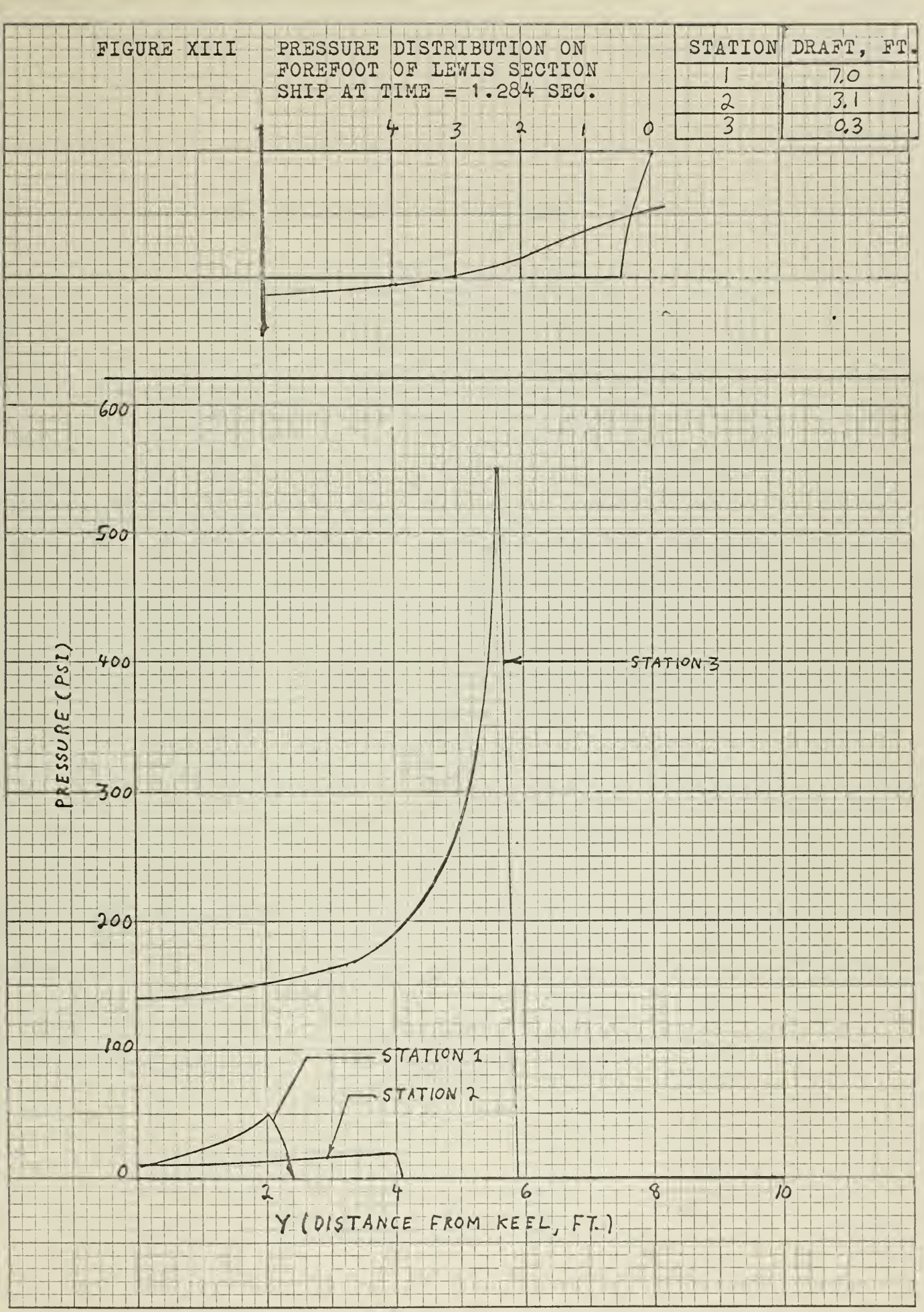

FIGURE XIV PRESSURE DISTRIBUTION ON FOREFOOT OF LEWIS SECTION SHIP AT TIME = 1.300 SEC.

STATION	DRAFT, FT.
1	7.6
2	3.8
3	0.8

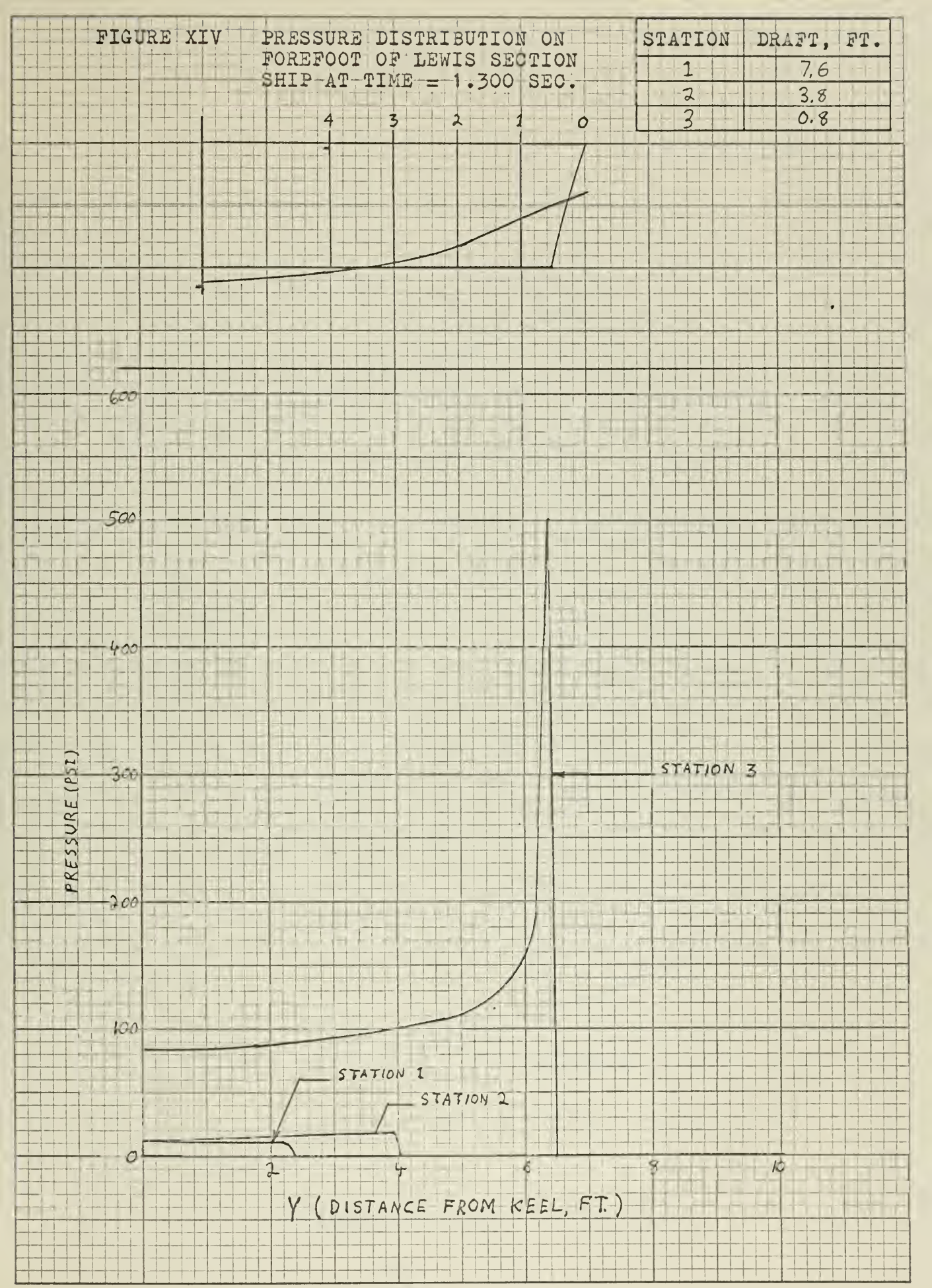

FIGURE XV PRESSURE DISTRIBUTIO ON FOREFOOT OF LEWIS SECTION SHIP AT TIME = 1.375 SEC.

STATION	DRAFT, FT.
1	10.5
2	6.4
3	3.0
4	0.8

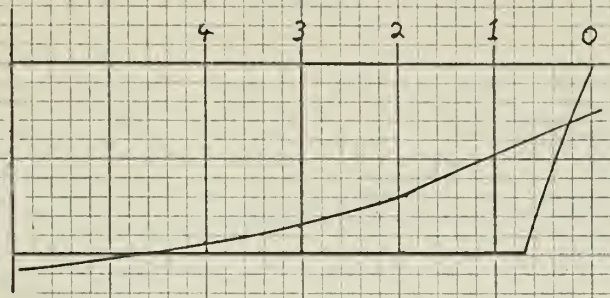

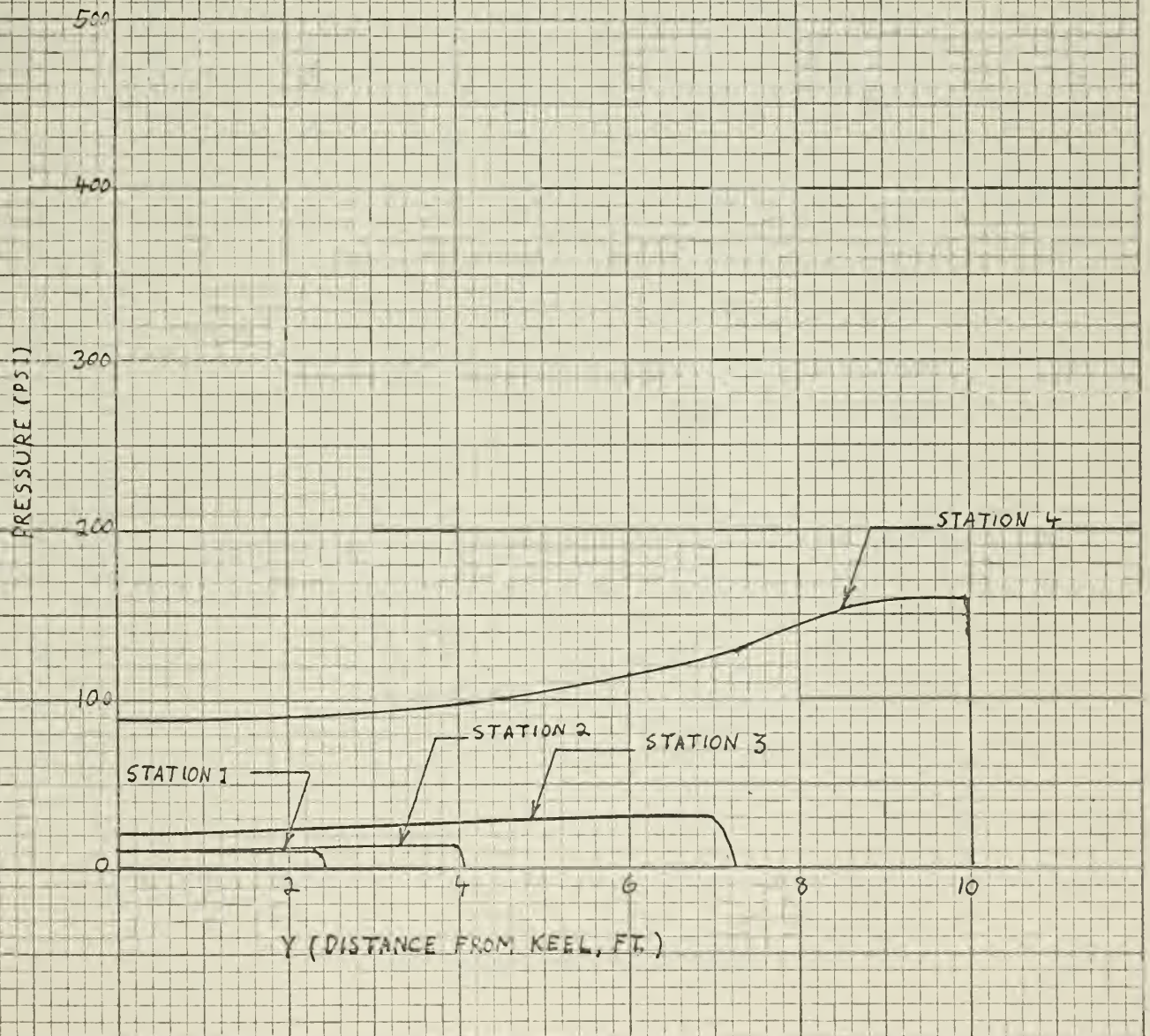

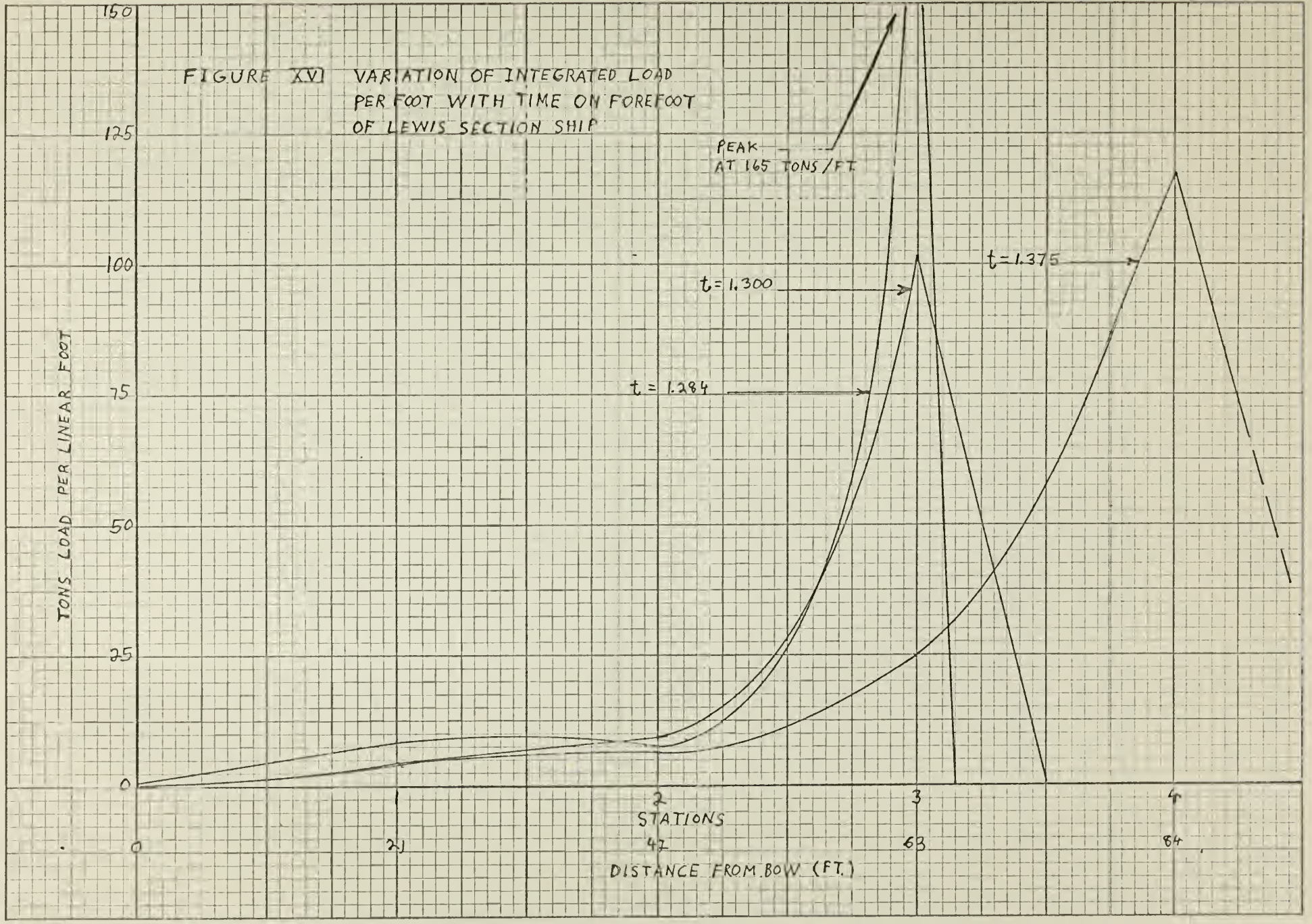
FIGURE XVI VARIATION OF INTEGRATED LOAD PER FOOT WITH TIME ON FOREFOOT OF LEWIS SECTION SHIP
PEAK AT 165 TONS/FT.
t = 1.375
t = 1.300
t = 1.284
TONS LOAD PER LINEAR FOOT
150
125
100
75
50
25
0
0
21
47
63
84
1
2
3
4
STATIONS
DISTANCE FROM BOW (FT.)

FIGURE XVII COMPARISION OF EXPANDING PLATE THEORY AND WEDGE FREE SURFACE ANALYSIS

STATION	DRAFT, FT.
2	0.3

— — — Pressure distribution on station 2 of Liberty ship from DTMB 913 computed by expanding plate theory

——— Pressure distribution computed by free surface analysis - approximated by wedge, β = 20 degrees

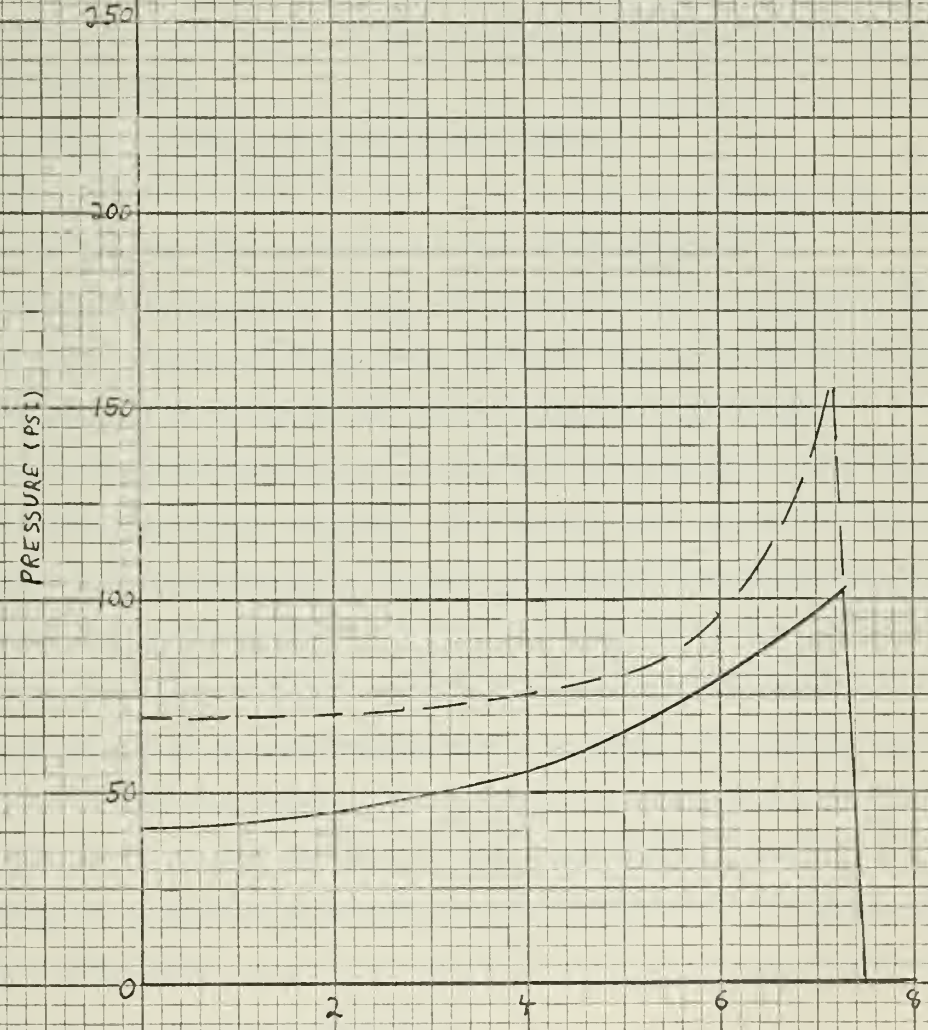

IV DISCUSSION OF RESULTS

A. Introduction

Before discussing the results, the theoretical assumptions made will be restated.

1) Only two dimensional sections were considered.
2) Each impacting section was assumed to be perfectly rigid, and to be symmetrical about the centerline plane.
3) While the velocity of penetration was not constant, for the small time interval under consideration, it was considered to vary linearly and average values were used.
4) The flow field is assumed to be irrotational.
5) The fluid is considered to be frictionless and incompressible, and the effects of gravity and surface tension are neglected.
6) On the basis of irrotational flow, the particles of the original surface are considered to remain in the free surface. The surface deflected by the impacting body is assumed to have a constant arc length.
7) The theoretical procedure was based on a mathematical model of a wedge with constant entry velocity. The theory was applied to the water entry of actual ship sections by assuming that the impacting sections were approximately blunt nose wedges. That is, the free surface formed during the initial impact stages was considered to be equivalent to that formed by a wedge of an equivalent deadrise angle. The spray was considered to shoot off at an angle determined by the slope of the hull at the wetted width. For the hull sections where the deadrise angle was approximately zero, the velocity potential was determined by the expression for flow along a flat plate.

IV DISCUSSION OF RESULTS

A. Introduction

Before discussing the results, the theoretical assumptions made will be restated.

1) Only two dimensional sections were considered.

2) Each impacting section was assumed to be perfectly rigid, and to be symmetrical about the centerline plane.

3) While the velocity of penetration was not constant, for the small time interval under consideration, it was considered to vary linearly and average values were used.

4) The flow field is assumed to be irrotational.

5) The fluid is considered to be frictionless and incompressible, and the effects of gravity and surface tension are neglected.

6) On the basis of irrotational flow, the particles of the original surface are considered to remain in the free surface. The surface deflected by the impacting body is assumed to have a constant arc length.

7) The theoretical procedure was based on a mathematical model of a wedge with constant entry velocity. The theory was applied to the water entry of actual ship sections by assuming that the impacting sections were approximately blunt nose wedges. That is, the free surface formed during the initial impact stages was considered to be equivalent to that formed by a wedge of an equivalent deadrise angle. The spray was considered to shoot off at an angle determined by the slope of the hull at the wetted width. For the hull sections where the deadrise angle was approximately zero, the velocity potential was determined by the expression for flow along a flat plate.

8) The ship motion expressions were determined experimentally for a Liberty ship of approximately the same dimensions as the ship found from Lewis sections.

B. Determination of Pressure Distributions

The ship motion expression for the relative velocity did not include the effect of ship forward speed. For a small pitch angle, the total relative normal velocity of the keel is:

$$V_n = U\psi + X\dot{\psi} + \dot{z} - \dot{r}$$

where U is the effect of the forward speed on the normal velocity. If the pitch angle is small at the instant of slamming, U can be safely neglected. At t = 1.284 sec., the first time for calculations, the pitch angle was approximately 0.2° . Therefore, the contribution of U to the relative velocity was not important.

Figures XIII to X V represent the pressure distribution on the forefoot of the ship at approximately the time of slamming. The pressures were computed for all stations from 1 to 5 which are immersed at the particular time. The pressure distributions are not really sufficient to give a definite value to the maximum pressure to which the ship is subjected.

The pressure distribution curves are similar to the curves obtained in reference (3) for the Liberty ship. While the peaks on the curves obtained in this paper were lower, this is probably not significant. The peak pressures are of extremely short duration, and are relatively unimportant. For example, at t = 1.270 station 3 was out of the water, but .0184 sec. later it had a peak pressure of 550 psi at y = 5.8' , and .016 sec. later there was a pressure of approximately 120 psi at y = 5.8' . However, it does seem that the average pressure distribution at a station varies directly as the peak pressure.

3) The ship motion expressions were determined experimentally for a Liberty ship of approximately the same dimensions as the ship tested from Lewis sections.

B. Determination of Pressure Distributions

The ship motion expression for the relative velocity did not include the effect of ship forward speed. For a small pitch angle, the total relative normal velocity of the keel is:

$$V_n = U\psi + \dot{X}\psi + \dot{z} - \dot{\zeta}$$

where U is the effect of the forward speed on the normal velocity. If the pitch angle is small at the instant of slamming, U can be safely neglected. At t = 1.284 sec., the first time for calculations, the pitch angle was approximately 0.8°. Therefore, the contribution of U to the relative velocity was not important.

Figures XII to XV represent the pressure distribution on the forefoot of the ship at approximately the time of slamming. The pressures were computed for all stations from 1 to 5 which are immersed at the particular time. The pressure distributions are not really sufficient to give a definite value to the maximum pressure to which the ship is subjected.

The pressure distributed curves are similar to the curves obtained in reference (3) for the Liberty ship. While the peaks on the curves obtained in this paper were lower, this is probably not significant. The peak pressures are of extremely short duration, and are relatively unimportant. For example, at t = 1.370 station 3 was out of the water, but .0126 sec. later it had a peak pressure of 830 psi at $\dot{y} = 11.8'$, and .016 sec. later there was a pressure of approximately 130 psi at $\dot{y} = 5.3'$. However, it does seem that the average pressure distribution at a station varies directly as the peak pressure.

An attempt was made to determine the pressure at station 3 at a slightly earlier time, but the construction of the free surface was extremely difficult to perform, and the author had no reason to believe the results were correct. It is quite possible, however, that the peak pressure might be even higher at station 3 at an earlier instant of time.

Referring to Figure XVII the pressures on station 2 of the Liberty ship were uniformly lower than those determined in reference (3) by the expanding plate theory. This result is probably the more accurate, since the ship section could accurately be represented by a wedge during the time of initial entry into the water. The wedge assumption would not have been valid at a draft of 6 ft., or greater, but by this time the impact pressures have been greatly reduced. From the results given in reference (7), it is to be expected that the computation of pressure distributions on wedge-shaped bodies, by considering the free surface, will give somewhat lower pressures than those calculated by the expanding plate theory.

The integrated slamming load distribution in tons/ft. of length, is shown in Figure XVI. At best, these curves are crude approximations, since each curve was determined by only 3 or 4 points. A much better method would be to compute the pressure distribution at $\frac{1}{2}$ and $\frac{1}{4}$ stations in the area of slamming. This was not done in this paper since the offsets for fractional stations were not available. However, even with the points available, a good idea can be obtained as to the total slamming load on the forefoot of the ship at the indicated times.

An attempt was made to determine the pressure at station 3 at a slightly earlier time, but the construction of the free surface was extremely difficult to perform, and the author had no reason to believe the results were correct. It is quite possible, however, that the peak pressure might be even higher at station 3 at an earlier instant of time.

Referring to Figure XVII the pressures on station 8 of the Liberty ship were uniformly lower than those determined in reference (3) by the expanding plate theory. This result is probably the more accurate, since the ship section could accurately be represented by a wedge during the time of initial entry into the water. The wedge assumption would not have been valid at a draft of 8 ft., or greater, but by this time the impact pressures have been greatly reduced. From the results given in reference (7), it is to be expected that the computation of pressure distribution on wedge-shaped bodies, by considering the free surface, will give somewhat lower pressures than those calculated by the expanding plate theory.

The integrated slamming load distributions in tons/ft. of length, is shown in Figure XVI. At best, these curves are crude approximations, since each curve was determined by only 3 or 4 points. A much better method would be to compute the pressure distribution at $\frac{1}{8}$ and $\frac{1}{4}$ station in the area of slamming. This was not done in this paper since the offsets for fractional stations were not available. However, even with the points available, a good idea can be obtained as to the total slamming load on the forefoot of the ship at the indicated times.

V. CONCLUSIONS

1) The method of analysis given in this paper is at least a reasonable approximation since the curves of pressure distribution are of the correct shape.

2) The procedure for determining the pressure distribution by considering the free surface shape is a long and tedious process. There are inherent sources of error in the construction of the free surface, and in the graphical and numerical solutions for the pressures, even for a simple wedge. The procedure, when adapted to a ship form, is even more questionable. However, there does seem to be some merit in the procedure, and it is concluded that it can be refined considerably. The biggest improvement would be to develop a computer solution for the procedure.

3) The wave rise is probably accurately given for an impacting body by either equation (3) or (27), depending on the shape of the body. However, it is evident that equation (8) cannot be used to determine the spray root thickness for a ship section. When the free surface was constructed for the blunt nosed sections, the spray root thickness had to be estimated. This was possibly a large source of error.

4) The determination of the free surface shape in the spray root area is quite critical. This is where the particle velocities are the highest, and even a small error in the shape results in a large error in directions and magnitude of particle velocities. However, even with the possible sources of error in the spray root region, the pressures actually obtained for this region were as realistic as those determined by expanding plate theory.

V. CONCLUSIONS

1) The method of analysis given in this paper is at least a reasonable approximation since the curves of pressure distribution are of the correct shape.

2) The procedure for determining the pressure distribution by considering the free surface shape is a long and tedious process. There are inherent sources of error in the construction of the free surface, and in the graphical and numerical solutions for the pressures, even for a simple wedge. The procedure, when adapted to a ship form, is even more questionable. However, there does seem to be room for improvement in the procedure, and it is concluded that it can be refined considerably. The biggest improvement would be to develop a computer solution for the procedure.

3) The wave rise is probably accurately given for an impacting body by either equation (3) or (37), depending on the shape of the body. However, it is evident that equation (8) cannot be used to determine the spray root thickness for a ship section. When the free surface was constructed for the flat panel section, the spray root thickness had to be estimated. This was possibly a large source of error.

4) The determination of the free surface shape in the spray root area is quite critical. This is where the parabolic velocities are the largest, and even a small error in the shape results in a large error in direction and magnitude of vertical velocities. However, even with the possible sources of error in the spray root region, the pressures actually obtained for this region were as realistic as those determined by expanding plate theory.

5) The procedure described in this paper is only valid during the initial impact, and a short time afterward. After the body has penetrated to a sizeable depth, the effect of gravity, and spray dissipation, will render consideration of the free surface useless. However, the highest pressures will, of course, occur at the time of impact or immediately afterward, when the added mass of the body is changing most rapidly.

5) The procedure described in this paper is only valid during the initial impact, and a short time afterward. After the body has penetrated to a sizeable depth, the effect of gravity, and spray dissipation, will render consideration of the free surface useless. However, the highest pressures will, of course, occur at the time of impact or immediately afterward, when the added mass of the body is changing most rapidly.

VI. RECOMMENDATIONS

1) Experimental and additional theoretical work should be performed to determine if similarity principles can be applied to ship sections of general shape. Particular attention should be given to determining how the expansion of the free surface is determined by the shape of the impacting body. As a start, experiments could be devised which utilized impacting wedges of various deadrise angles and a high speed camera. The spray root thickness and the angle at which the spray leaves the body should be thoroughly investigated.

2) Computer procedures should be developed for the solution of hydrodynamic impact problems involving a non-zero velocity potential free surface.

3) Accurate theoretical and experimental methods should be developed which will give the total slam load acting on the forefoot of the ship at any instant of time.

4) The effects on slamming loads of hull flexibility and water compressibility should be investigated both theoretically and experimentally.

VI. RECOMMENDATIONS

1) Experimental and additional theoretical work should be performed to determine if similarity principles can be applied to ship sections of general shape. Particular attention should be given to determining how the expansion of the free surface is determined by the shape of the impacting body. As a start, experiments could be devised which utilized impacting wedges of various deadrise angles and a high speed camera. The spray root thickness and the angle at which the spray leaves the body should be thoroughly investigated.

2) Computer procedures should be developed for the solution of hydrodynamic impact problems involving a non-zero velocity potential free surface.

3) Accurate theoretical and experimental methods should be developed which will give the total slam load acting on the forefoot of the ship at any instant of time.

4) The effects on slamming loads of hull flexibility and water compressibility should be investigated both theoretically and experimentally.

VII. APPENDIX

A. Sample Calculations

B. Literature Citations

APPENDIX A

Sample Calculations U-Shaped Section (Lewis Ship, Station 3), t = 1.284 sec.)

The first estimate of the surface shape is computed by using equations (27), and the continuity principle. From the plotting of the wave rise, the wetted width (c) is determined to be 5.95 ft. (See Figure A-I). The slope of the hull section at y = c is determined to be approximately 63° . This is the angle at which the spray is assumed to shoot off. The spray tip, 0' , is located by measuring along the wave and wedge from y = 10' a distance s = y = 10' . (At the distance y = 15' , the wave slope is quite small, so that s = y is a close approximation.) A spray thickness of $\delta/c = .12$ was assumed. Once the spray and wave have been merged together, the spray tip is located more exactly by following the curved surface (0' is located on the line drawn tangent to the hull at y = c, at an angle of $\beta = 63°$). The area of the displaced water above the original water line is made to equal the area of the submerged body below the original water line. Then equations (6) are used to check the position of the water particles. The steps of the numerical integration for the surface shape are shown in Table II. The new particle positions were determined by the following approximate forms of equations (6):

$$\eta\ (y)\ \text{new} = s_o \sum \frac{wt}{s^2} \quad \Delta s$$

$$\xi - \xi_o\ \text{new} = s_o \sum \frac{vt}{s^2} \quad \Delta s$$

APPENDIX A

Example Calculations U-Shaped Section (Lewis Flip, Series I), v_o = 1,366 fps)

The first estimate of the surface shape is computed by using equations (37), and the continuity principle. From the plotting of the wave rise, the wetted width (c) is determined to be 8.55 ft. (See Figure A-1). The slope of the hull section at $y = c$ is determined to be approximately 68°. This is the angle at which the spray is assumed to shoot out. The spray tip, 0', is located by measuring along the wave and wedge from $y = 10'$ a distance $s = y = 10'$. (At the distance $y = 16'$, the wave slope is quite small, so that $s = y$ is a close approximation.) A spray thickness of $\delta/c = .12$ was assumed. Once the spray and wave have been merged together, the spray tip is located more exactly by following the curved surface (0' is located on the line cross tangent to the hull at $y = c$, at an angle of $\alpha = 62°$). The area of the displaced water above the original water line is equal to the area of the submerged body below the original water line. Then equations (6) are used to check the position of the water particles. The steps of the numerical integration for the surface shape are shown in Table I. The new particle positions were determined by the following approximate forms of equations (8):

$$\Delta y \;(y)\; \text{new} = \frac{\Delta t}{M} \sum_{0}^{n} F_y \qquad \text{eq}$$

$$\Delta x \;(x)\; \text{new} = \frac{\Delta t}{M} \sum_{0}^{n} F_x \qquad \text{eq}$$

After the free surface shape has been determined, the velocity potential can be determined on the body. For the flat portion of the hull, from y = 0 to y = 4.7, the potential is determined by equation (28). In this computation, a is taken to be equal to the wetted width at the time under consideration, but the equation is only used for the flat portion of the hull (from y = 0 to y = 4.7).

For the portion of the hull (from y = 4.7 to y = 6.05) the velocity potential is computed by integrating the velocity along the hull surface. The tangential velocity (v_o) along the hull is determined from equation (17). Four points are chosen on the curved portion of the hull for the determination of the velocity (see Figure A-1). The iy and x axis are constructed tangent and perpendicular to the hull at each point under consideration. The velocity (v_o) is determined by equation (17) by numerical integration around the free surface:

$$v_o = \frac{1}{\pi}\sum v\,d\theta + \frac{1}{\pi}\sum u\,d(\ln R)$$

The steps in the integration are shown in Table III for point 2 (z, v, and u refer to the position and velocities of points on the free surface). On the body, v_o is equal to $z_x \cos\beta$ at any point. Knowing the component velocities, the resultant velocity (U) can be found at any point. The velocities and velocity potential determined at the points on the hull, shown in Figure A-I, are listed in Table IV.

Now the pressure can be determined for equation (24):

$$\frac{p}{\rho} = -\frac{\phi}{t} + \frac{r}{t} U\cos\alpha - \frac{U^2}{2}$$

where is the distance from the origin to the point on the body under consideration, and α is the angle between and U. The results of the solution of equation (24) for station 3 at t = 1.284 are listed in Table IV. The time, t, involved in equation (24) is the elapsed time from impact

of the body. For the case under consideration, t_o (impact time) = 1.270, and the computations were carried out from time t_1 = 1.284 sec. Therefore, $t = t_1 - t_o$ = .014 sec. in equation (24).

of the body. For the case under consideration, t_0 (impact time) = 1.310, and the computations were carried out from time t_1 = 1.188 sec. Therefore, $\Delta = t_1 - t_0 = -.012$ sec. in equation (16).

TABLE II

NUMERICAL INTEGRATION FOR SURFACE SHAPE

Station 3 $t = 1.284$ $z_x = 0.3$ $\dot{z}_x = 26.0$ $\beta = 63°$

s	η_{start}	wt	$\frac{wt}{s^2}$	$\frac{wt}{s^2}\Delta s$	$\sum\frac{wt}{s^2}\Delta s$	η_{new}	α	Ut
10	.13	.15	.001		.013	.13	90	.15
				.0025				
9	.14	.30	.004		.016	.14	90	.30
				.007				
8	.17	.60	.009		.022	.18	88	.60
				.015				
7	.24	1.00	.021		.037	.25	85	1.00
				.017				
6.5	.31	1.90	.045		.054	.35	79	1.90
				.018				
6.25	.45	4.00	.103		.080	.50	69	4.20
				.026				
6.05	.59	5.80	.154		.106	.64	55	6.70
				.026				
5.9	.71	6.50	.187		.132	.77	45	8.30
				.037				
5.7	.89	6.00	.184		.169	.96	27.5	10.55
				.038				
5.5	1.09	6.00	.198		.207	1.15	25.3	10.55

Area of submerged body = 1.54 ft

Area of displaced water = 1.60 ft

s	$\xi - \xi_o)_{start}$	vt	$\frac{vt}{s^2}$	$\frac{vt}{s^2}\Delta s$	$\sum\frac{vt}{s^2}\Delta s$	$\xi_{new} - \xi_o$
10	0	0	0		0	0
9	0	0	0		0	0
8	0	0	0		0	0
7	.04	.08	.0016		0	0
				.004		
6.5	.07	.25	.006		.004	.03
				.005		
6.25	.09	1.30	.033		.009	.06
				.012		
6.05	.18	3.30	.090		.021	.13
				.018		
5.9	.30	5.20	.149		.039	.24
				.042		
5.7	.53	8.70	.268		.081	.46
				.056		
5.5	.80	8.70	.288		.137	.75

TABLE III

Numerical Integration of Equation (17)

z	v	u	θ	vdθ	R	ln R	ud(ln R)
s = 10	10	- 5	.40		4.2	1.43	
				0			8.0
s = 8	38	- 20	.40		2.2	.79	
				- 8.			33.0
s = 6.5	129	- 42	.30		.75	- .29	
				163			3.4
s = 6.05	475	25	.84		.50	- .69	
				245			34.0
s = 5.70	666	354	1.27		.60	- .51	
				93			124
s = 5.50	666	354	1.41		.85	- .16	
				80			478
s = 3.0	666	354	1.53		3.3	1.19	
				27			230
s = 0	666	354	1.57				
				600			910

v_o (point 2) = $\frac{1}{\pi}(600) + \frac{1}{\pi}(910) = 481$ ft/sec

$u_o = \dot{z}_x \cos 63^\circ = 11.8$ ft/sec

TABLE IV

Velocity, Velocity Potential, and Pressure Distribution on Station 3 of Lewis Ship(t = 1.284 sec)

y	ϕ (ft^2/sec)	v_o (Flat Plate)	v_o (Cauchy Integral)	u_o	p (psi)
0	-154.5	0	5	26.0	144
1	-152.0	4.43	6	26.0	145
2	-143.5	9.42	10	26.0	147
3	-134.0	15.16	17	26.0	165
4	-114.8	23.60	24	26.0	200
4.7	- 98.2	32.30	28	26.0	202
5.6	3.0		158	20.5	550
5.85	160		481	11.8	200

FIGURE A-I CONSTRUCTION OF FREE SURFACE FOR STATION 3 OF LEWIS SECTION SHIP AT $t = 1.284$ SEC.

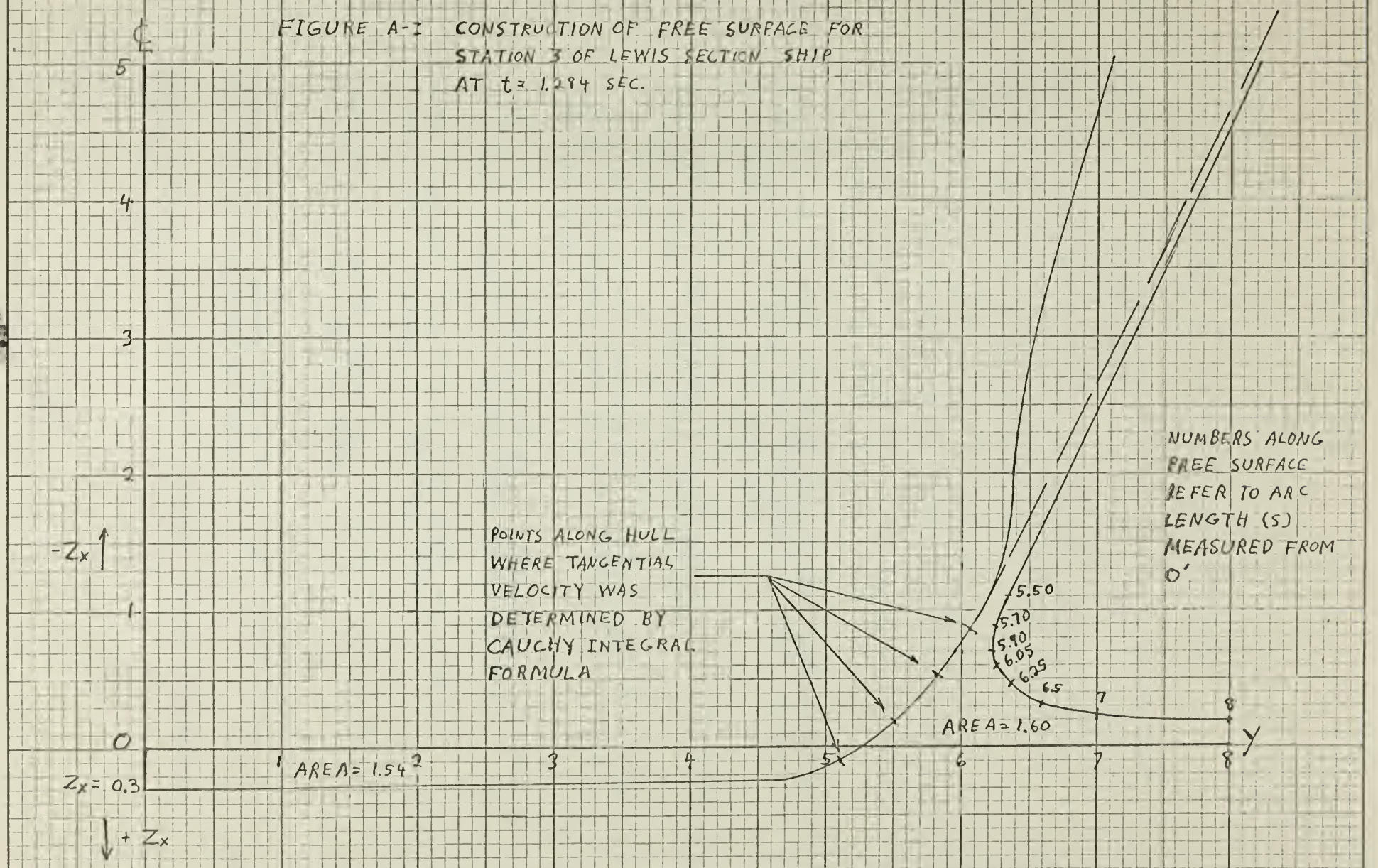

APPENDIX B LITERATURE CITATIONS

1. Von Karman, "The Impact on Seaplane Floats During Landing", N.A.C.A., T. N. 321, 1929;

2. Chu, Wen-Hwa, and Abramson, H. Norman, "Hydrodynamic Theories of Ship Slamming-Review and Extention", Journal of Ship Research, Vol. 4, No. 4, March 1961;

3. Szebehely, V. G., and Todd, M. A., "Ship Slamming in Head Seas", David Taylor Model Basin Report 913, February 1955;

4. Todd, M. A., "Slamming Due to Pure Pitching Motions", David Taylor Model Basin Report 833, January 1955;

5. Szebehely, V. G., and Lum, S. M. Y., "Model Experiments on The Slamming of a Liberty Ship in Head Seas", David Taylor Model Basin Report 914, February 1955;

6. Ochi, Kazuo, "Model Experiments on Ship Strength and Slamming in Regular Waves", Transactions, SNAME, 1953;

7. Pierson, J. D., "The Penetration of a Fluid Surface by a Wedge", Institute of Aeronautical Sciences, Fairchild Fund Preprint No. FF-3, July 1950;

8. Bledsoe, M. D., "Series Investigation of Slamming Pressures", David Taylor Model Basin Report 1043, December 1956;

9. Lewis, Frank M., "The Inertia of the Water Surrounding a Vibrating Ship", Transactions, SNAME, 1929;

10. Weinblum, G., and St. Denis, M., "On The Motions of Ships at Sea", Transactions, SNAME, 1950;

11. Szebehely, V. G., and Lum, S. M. Y., "Model Experiments on Slamming of a Liberty Ship in Head Seas", David Taylor Model Report 914, February 1955;

12. Lamb, Horace, "Hydrodynamics", 6th Ed., Dover Publications, New York, 1945;

APPENDIX B LITERATURE CITATIONS

1. Von Karman, "The Impact on Seaplane Floats During Landing", N.A.C.A., T. N. 321, 1929;

2. Chu, Wen-Hwa, and Abramson, H. Norman, "Hydrodynamic Theories of Ship Slamming-Review and Extension", Journal of Ship Research, Vol. 4, No. 4, March 1961;

3. Szebehely, V. G., and Todd, M. A., "Ship Slamming in Head Seas", David Taylor Model Basin Report 813, February 1952;

4. Todd, M. A., "Slamming Due to Pure Pitching Motions", David Taylor Model Basin Report 683, January 1958;

5. Szebehely, V. G., and Lum, K. M. Y., "Model Experiments on The Slamming of a Liberty Ship in Head Seas", David Taylor Model Basin Report 814, February 1958;

6. Ochi, Kazuo, "Model Experiments on Ship Strength and Slamming in Regular Waves", Transactions, SNAME, 1958;

7. Pierson, J. D., "The Penetration of a Fluid Surface by a Wedge", Institute of Aeronautical Sciences, Fairchild Fund Preprint No. FF-3, July 1956;

8. Bledose, M. D., "Series Investigation of Slamming Pressures", David Taylor Model Basin Report 1043, December 1956;

9. Lewis, Frank M., "The Inertia of the Water Surrounding a Vibrating Ship", Transactions, SNAME, 1929;

10. Weinblum, G., and St. Denis, M., "On The Motions of Ships at Sea", Transactions, SNAME, 1950;

11. Szebehely, V. G., and Lum, K. M. Y., "Model Experiments on Slamming of a Liberty Ship in Head Seas", David Taylor Model Report 814, February 1958;

12. Lamb, Horace, "Hydrodynamics", 6th Ed., Dover Publications, New York, 1945;

13. Pierson, John D., "On the Pressure Distribution for a Wedge Penetrating a Fluid Surface", ETT Report No. 336, Sherman M. Fairchild Publication Fund Paper No. 167, Institute of Aeronautical Science, New York;

14. Bisplinghoff, R. L., and Doherty, C. S., "A Two-Dimensional Study of the Impact of Wedges on a Water Surface", Aeroelastic and Structures Research, MIT Contract No. a(5)-9921, March 1950;

15. Hildebrand, F. B., "Introduction to Numerical Analysis", McGraw-Hill Book Co., 1956;

16. Sokolnikoff, I. S., and Redheffer, R. M., "Mathematics of Physics and Modern Engineering", McGraw-Hill Book Company, 1958;

17. Borg, S. F., "Some Contributions to the Wedge Water Entry Problem", Journal of Engineering Mechanics Division, Proceedings ASCE, Vol. 83, EM2, April 1957;

18. Szebehely, V. G., "Hydrodynamics of Slamming of Ships", David Taylor Model Basin Report 823, July 1953;

19. Milne-Thomson, L. M., "Theoretical Hydrodynamics", 4th Ed., Macmillan Company, New York, 1960.

18. Pierson, John D., "On the Pressure Distribution for a Wedge Penetrating a Fluid Surface", ASTA Report No. 326, Institute of Mathematical Sciences, New York University, 1967.

19. Sieglinde, E. L., and Doherty, G. S., "A Two-Dimensional Study of the Impact of Wedges on a Water Surface", Aeronautical and Structures Laboratory, MIT Contract No. N(3)-1221, March 1960.

20. Milne-Thomson, L. M., "Theoretical Hydrodynamics", 4th Ed., Macmillan Company, New York, 1960.

thesS924
Theoretical investigation of slamming lo
3 2768 002 06017 0
DUDLEY KNOX LIBRARY